中文摘要

Grb2 SH2 蛋白在Ras 致癌基因的訊息傳導途徑中扮演重要的角色，而在細胞的增生及分化影響甚大。所以我們專注在研發並建立一系列的胜肽抑制物來阻斷Grb2 SH2 蛋白的訊息傳遞進而達到抗癌的效果。然而細胞膜的屏障可能降低了設計胜肽的活性，為了增進其體外生物活性，針對胜肽之氨基酸序列作了一些修飾；因此RGD (Arg-Gly-Asp) 三胜肽的設計希望可以增加前導胜肽(Fmoc-Glu-Tyr-Aib-Asn-NH_2)的細胞通透性，進而達到抑制細胞內Grb2 SH2蛋白的活性。

*Myo*D 蛋白是DNA 結合蛋白它具有HLH 區塊的蛋白有特殊的交互作用形成homodimers 或hetrodimers，並且具有結合特異基因Id 蛋白質的穩定型式。Id 蛋白質家族包括四種相關的蛋白質，形成雙體則有高度穩定性而且是DNA結合蛋白質的抑制物，屬於抑制DNA與轉錄因子結合的蛋白質家族。Id 蛋白質家族包含一個高度保留的helix-loop-helix (HLH)雙體區塊。在訊息傳遞途徑中，Id扮演轉錄因子basic helix-loop-helix 家族之拮抗物(antagonist)的角色，在細胞生長、細胞增生、以及細胞分化方面扮演重要的角色。我們以*Myo*D 蛋白為藍本設計一系列對Id 蛋白具有高親和性的胜肽，期望這些胜肽可以干擾Id 蛋白與*Myo*D 蛋白或者與其他bHLH蛋白的結合而進一步達到抑制癌細胞增生的能力。

本研究應用SPR技術所發展的生物感測器（BIACORE 3000）鑑定設計胜肽對Grb2 SH2 蛋白之親和力，以及設計胜肽對Id1蛋白之親和力。而胜肽的二級結構的鑑定則是應用圓二色光譜儀進行研究。另外本研究亦培養不同的腫瘤細胞株並以胜肽處理後，評估胜肽對癌細胞之影響。最後，胜肽的生物活性測試我們也選擇了以流式細胞儀進行癌細胞的細胞週期的鑑定。

研究結果發現設計胜肽**2** (H-Arg-Gly-Asp-Glu-Tyr-Aib-Asn-Arg-Gly-Asp-NH2)對Grb2 SH2 蛋白具有較高的親和力並且對於乳癌細胞，MCF-7 and MDA-MB-453 cells, 百分之五十抑制濃度則分別為45.7 μM 及 47.4 μM；並且，經過此胜肽處理

過後的癌細胞其sub-G1細胞週期有明顯的增加。胜肽**3C** (H-Tyr-Ile-Glu-Gly-Leu-Gln-Ala-Leu-Leu-Arg-Asp-Gln-NH_2)則不但對Id1具有不錯的高親和力並且針對乳癌(MCF-7, MDA-MB-231)及大腸癌細胞(HT-29)的抗增生效果亦達到IC_{50}為25 μM。經過此胜肽僅5 μM處理過後的癌細胞其sub-G1細胞週期有明顯的增加。

由以上結果顯是我們所設計之胜肽不論是針對抑制Ras 致癌基因的訊息傳導途徑中的Grb2 SH2 蛋白以及針對干擾Id1 形成雙具體的目的，都具有顯著性的效果。此一結果可作為日後開發抗癌細胞增生的藥物藍本。

Abstract

The growth factor receptor-bound protein-Src homology 2 (Grb2 SH2) plays an important role in the oncogenic Ras signaling pathway, which involves in cell proliferation and differentiation. Therefore, we focus on developing peptidic inhibitors of the Grb2 SH2 domain as promising anticancer agents. However, cell membrane constitutes a serious barrier for protecting the integrity of cells, it may limit the effectiveness of peptidic inhibitors as anti-cancer drugs. In order to enhance the cell permeability of peptides, we designed the peptide analogs by incorporation of the cell-penetrating peptide (RGD tripeptide) into our leading peptide inhibitors of Grb2 SH2, Fmoc-Glu-Tyr-Aib-Asn-NH_2.

MyoD is a DNA binding protein capable of specific interactions specifically involved the helix-loop-helix (HLH) domain. The HLH motif of MyoD could form oligomers with the HLH motif of Id1 (the inhibitor of DNA-binding proteins) that folds into a highly stable helical conformation stabilized by the self-association. The Id family consists of four related proteins that contain a highly conserved dimerization motif known as act as dominant negative antagonists of the basic helix–loop–helix (bHLH) family of transcription factors which play important roles in cellular development, proliferation, and differentiation. We design and synthesize peptide fragments of MyoD with high affinity for Id1 in order to interrupt the interactions among Id1, MyoD and other bHLH DNA-binding proteins and to inhibit the proliferation of cancer cells.

The binding interaction between each synthetic peptide and Grb2 SH2 domain and affinity of each peptide for Id1 was determined by surface plasmon resonance (SPR) technology developed with the BIAcore-biosensor. The secondary structure of each peptide was studied by circular dichroism (CD) spectroscopy. Biological effects of each peptide in several cancer cells such as breast and colon cancer cells were analyzed. Effects of peptides on the cell cycle progression and apoptosis in cancer cell were

studied by flow cytometry.

Our results demonstrated that peptide analog **2** (H-Arg-Gly-Asp-Glu-Tyr-Aib-Asn-Arg-Gly-Asp-NH_2) for inhibiting Grb2 SH2 pathway had anti-proliferative effects on MCF-7 and MDA-MB-453 cells with an IC_{50} of 45.7μM and 47.4 μM, respectively. The cytotoxicity and percentage of sub-G1 in the cell cycle were increased in these cancer cells. And the peptide **3C** (H-Tyr-Ile-Glu-Gly-Leu-Gln-Ala-Leu-Leu-Arg-Asp-Gln-NH_2) not only showed high affinity for Id1, but also exhibited antiproliferative effects in HT-29 and MCF-7 cancer cells, the IC_{50} value of **3C** was determined as 25 μM in both cells. The percentage of sub-G1 in the cell cycle of the cancer cells treated with 5 μM of **3C** was increased.

Taken together, the peptides we designed for anti-Grb2 SH2 process and for interfering the dimerization of bHLH and Id1 were a promising lead compound for the development of antiproliferative agents.

Contents

Abbreviations

3D-QSAR	three-dimensional quantitative structure-activity relationship
bHLH	basic helix–loop–helix
CD	circular dichroism
CPP	cell-penetrating peptide
DIEA	N, N-diisopropylethylamine
DMEM	Dulbecco's modified eagle medium
DMF	dimethylformamide
EDC	1-ethyl-3(3-dimethyl aminopropyl) carbodiimide
EMSA	electrophoretic mobility shifts assay
FACS	fluorescence-activated cell sorting
FITC	fluorescein isothiocyanate
Grb2	growth factor receptor bound protein 2
HBS	hepes buffered saline
HBTU	2-(1H-benzotriazoleiyl)-tetramethyluronium hexafluorophosphate
HER-2	human epidermal growth factor receptor-2
HLH	helix–loop–helix
HOBt	1-hydroxybenzotriazole
IC50	the half maximal inhibitory concentration
Id	the inhibitor of DNA-binding proteins
K*D*	dissociation equilibrium constant
LDH	lactate dehydrogenase
MALDI-TOF-MS	matrix-assisted laser desorption/ionization time of flight mass spectrometer
MTT	3-(4,5-Dimethylthiazol-2-yl)-2,5-diphenyltetrazolium bromide
MyoD	myogenic differentiation protein
NHS	N-hydroxysuccinimide
PBS	phosphate buffered saline
pTry	phosphotyrosine
RGD	Arg-Gly-Asp
RP-HPLC	reversed phase high-performance liquid chromatography
RU	resonance unite
SE	sedimentary equilibrium
SH2	Src homology 2
SH3	Src homology 3
SPPS	solid phase peptide synthesis
SPR	surface plasmon resonance
TFA	trifluoroacetic acid

List of tables

List of figures

Figure 1-8. Time and dose-dependent curves for RGD in the MTT reduction assay. Human breast cancer cells MCF-7 and MDA-MB-453 were treated with RGD tripeptide for 24 hrs. The data shown represent the mean ± SEM of the mean cell counts from three independent experiments performed and analyzed as described.

Figure 1-9. Time and dose-dependent curves for peptide **2** in the MTT reduction assay. Human skin cells HS-68 were treated with 0, 25, 50, 75 and 100 μM of peptide **2** for 24 and 48 hrs. The data shown represent the mean ± SEM of the mean cell counts from three independent experiments performed and analyzed as described.

Figure 1-10. Dose-response curve of cytotoxicity was determined by the LDH assay of peptide **2**-treated breast cancer cells.
* Significant different at $p < 0.05$ level as compared with medium control. Data are presented as the mean ± SD (n = 3)

Figure 1-11. Effects of peptide **2** on cell cycle of breast cancer cell lines. The cells were incubated with 100 μM of peptide **2** for 24 h, and they were harvested and analyzed by flow cytometry.

Figure 2-1. Proposed mechanism of the inhibitory effect of a designed peptide on MyoD-Id1 interactions. (A) A heterodimer of the E2A proteins and MyoD mediates the DNA binding. (B) The inhibitor of DNA binding protein (Id1) forms the Id1/E2A or Id1/MyoD heterodimer to control the gene expression. Id exerts its dominant negative effect on sequestering the ubiquitously expressed MyoD. (C) Our proposed mechanism for interrupting the Id1 functions by the designed peptide. We propose that the association/interaction of the designed peptide with Id1 should interrupt the binding of Id to bHLH family, leading to the inhibitory effect on the proliferation of cancer cells.

Figure 2-2. Designed peptide fragments of the bHLH (basic-helix-loop-helix) domain of MyoD. (A) Amino acid sequences of bHLH domain of MyoD; (B) amino acid sequences of peptides **1A**, **2A**, and **3A**.

Figure 2-3. An overlay plot of the binding curves showing the interactions of peptides **1A**, **2A** and **3A** with the immobilized Id1. Peptide solutions (50 μM in 10 mM HEPES, 0.5 mM $MnCl_2$, 0.5 M $CaCl_2$ and 0.05% surfactant, pH 7.4) were injected. The bound peptide was dissociated by 30 mM NaCl (20 μL/min).

Figure 2-4. Amino acid sequences of designed peptides **3A**, **3B**, **3C**, and **3D**.
In order to synthesize cyclic potent peptide for future structure-activity relationships study, the peptides **3B** and **3C** was designed with an additional Cys at the C-terminal of each peptide.

Figure 2-5. Analysis of binding affinity of the peptide 3C for the immobilized Id1 using surface plasmon resonance technology. (A) Representative sensorgrams of binding of different concentrations of peptide 3C (50, 25, 12.5, 6.25 and 3.125 μM) to the immobilized human Id1 which derived from a 1:1 binding model. From the global fits k_{on} = 959 $M^{-1}S^{-1}$, k_{off} = 0.0179 S^{-1}, and the K_D value was determined as 18.6 μM by using BIA-software. The X- and Y-axis of sensorgram are time (seconds) and resonance unit (RU); (B) Scatchard plot of the binding data determined the K_D value as 12.5 μM by plotting the RU/ [peptide concentration] versus RU, and then calculating the slope which is equal to $-1/K_D$. The X- and Y-axis of plot are RU and RU/ [peptide concentration].

Figure 2-6. The spectra of the synthesized peptides (**3A**, **3B**, **3C** and **3D**) detected by circular dichroism (CD) spectroscopy.

Figure 2-7. The cell viability of peptide-treated human colon cancer cells and breast cancer cells. (A) Human colon cancer cells HT-29 were treated with 100 μM of peptide **3A**, **3B, 3C,** and **3D** for 24 hrs; (B) Human colon cancer cells HT-29 were treated with 5, 20, 40, 60, and 80 μM of **3C** for 24 hrs and 48 hrs; (C) Human breast cancer cells MCF-7 were treated with 5, 20, 40, 60, and 80 μM of **3C** for 24 hrs and 48 hrs. The Cell viability of peptide-treated cancer cells was determined by the MTT assay. Data are the mean value ± SD (the standard deviation) of three independent experiments. $*p < 0.05$ compared with control.

Figure 2-8. The cell viability of peptide-treated human breast cancer cells. Human breast cancer cells MDA-MB-231 were treated with 5, 10, 20, 40, 60, and 80 μM of peptide **3C** for 24 hrs and 48 hrs. The cell viability of was determined by the MTT assay. Data are the mean value ± SD of three independent experiments. $*p < 0.05$ compared with control.

Figure 2-9. The cell viability of peptide-treated human skin cancer cells. Human skin cells HS-68 were treated with 0, 25, 50, 75 and 100 μM of the peptide **3C** for 24 hrs and 48 hrs. The cell viability of peptide-treated cells was determined by the MTT assay. Data are the mean value ± SD of three independent experiments.

Figure 2-10. Effects of peptide **3C** on the cell cycle of breast cancer cells (MCF-7). The cells were incubated with 5 μM of peptide **3C** for 24 hrs and 48 hrs, and then analyzed by flow cytometry. (A) The FACS profiles of MCF-7 cancer cells and cancer cells treated with **3C**; (B) Effect of **3C** on the distribution of MCF-7 cells in distinct phases in the cell cycle. MCF-7 cells were continuously exposed to **3C** at the indicated concentrations for 24 hrs or 48 hrs. The graph represents the mean value ± SD of two independent experiments.

Figure 2-11. Association to the Id1 ligand of six alanine replaced peptide **3C** analogs by SPR method in aqueous buffered solution (pH 7.5).

Chapter 1

Effects of peptidic antagonists of Grb2 SH2 on human breast cancer cells

Abstract

The growth factor receptor-bound protein Src homology 2 (Grb2 SH2) plays an important role in the oncogenic Ras signaling pathway, which involves in cell proliferation and differentiation. Therefore, the antagonist of Grb2 SH2 has become a potential target for developing anticancer agents. Recently, we discovered a peptide **1** (Fmoc-Glu-Tyr-Aib-Asn-NH2) with high affinity for the Grb2 SH2 domain by using surface plasmon resonance (SPR)-biosensor technology. Herein, we report the further design of the lead peptide **1** by addition of an Arg-Gly-Asp sequence to **1** to enhance binding to Grb2 SH2 and inducing apoptosis in cancer cells. Both the linear and cyclic analogs of the newly designed compound were prepared along with an analog in which the Nα-Fmoc group was removed. These peptide analogs were assayed for their affinity for the Grb2 SH2, their antiproliferative effect on human breast cancer cells, their specificity for cancer cells, and their effects on cytotoxicity and the cell cycle. MCF-7 and MDA-MB-453 breast cancer cells were treated with various concentrations of each peptide. The cell viability and cytotoxicity of peptide-treated cells were determined by using the cell proliferation kit (3-[4, 5-dimethyl-2-thiazolyl]-2, 5-diphenyl-tetrazolium bromide, MTT) and cytotoxicity kit (lactate dehydrogenase, LDH), respectively. Effects of peptides on the cell cycle progression of cancer cells and apoptosis were analyzed by using flow cytometry. Results demonstrated that the peptide analog **2** (H-Arg-Gly-Asp-Glu-Tyr-Aib-Asn-Arg-Gly-Asp-NH_2) had anti-proliferative effects on MCF-7 and MDA-MB-453 cells with an IC_{50} of 45.7 μM and 47.4 μM, respectively. The cytotoxicity and percentage of sub-G1 in the cell cycle were increased in these cancer cells when cells were treated with higher concentration of the Arg-Gly-Asp-containing peptide **2**. These results provide important information for the development of anti-cancer agents.

Introduction

The aberrant cell proliferation in breast cancer has been related to the abnormal function of cytoplasmic or receptor tyrosine kinase activities coupled to p21 Ras [1]. Oncoprotein overexpression of human epidermal growth factor receptor-2 (HER-2) is an important prognostic factor associated with breast cancer. Src homology 2 (SH2) domains play important roles in the signal transduction of HER-2 [2]. SH2 domains are relatively small protein modules of approximately 100 amino acids that recognize sequences containing pTyr (pY, phosphotyrosine), thereby expediting phosphorylation-dependent interactions of proteins results in signal propagation [3]. SH2 domains of proteins organize intracellular signaling by interacting with characteristic pTyr-containing proteins, activating distinct signaling pathways, and finally transducing signals initiated at growth factor receptors. SH2 domains are potential sites for the development of therapeutic agents [4], and considerable effort has been devoted to study the structural basis of SH2 domains binding to the pTyr-containing targets [5] and to develop peptides or peptidomimetics with high affinity for the SH2 domains [6-11].

The growth factor receptor bound protein 2 (Grb2) is an adaptor protein with a domain structure of SH3-SH2-SH3 [12]. It performs a principal role in the important Ras signal transduction pathway [13, 14], and rendering this protein an attractive target for the design of inhibitors as anticancer agents [15].

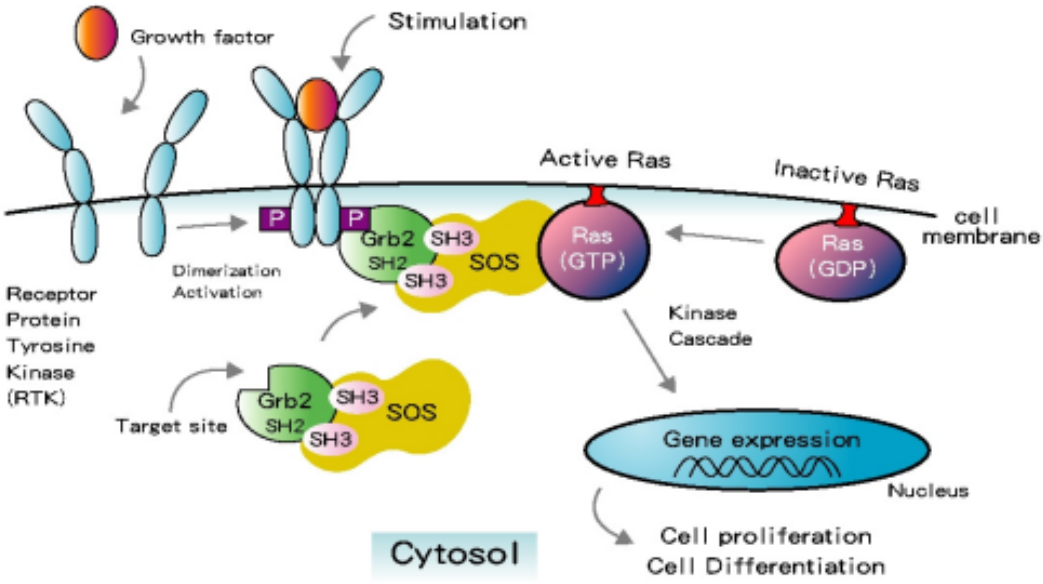

Ras signal pathway. Grb2 SH2 domains recognize sequences containing pTyr (pY, phosphotyrosine), thereby expediting phosphorylation-dependent interactions of proteins results in signal propagation and active the Ras system.

We have reported several potent small peptidic inhibitors of Grb2 SH2 that were analyzed by using the surface plasmon resonance (SPR) technology developed with the biosensor-BIACORE X instrument [16]. We also studied the structure-activity relationship of peptide **1**, Fmoc-Glu-Tyr-Aib-Asn-NH_2, and demonstrated that peptide **1** is the most potent peptide inhibitor of the Grb2 SH2 with an IC_{50} value of 8.7 μM [17, 18].

The objective of this study was to investigate the antiproliferative effects of the leading peptide **1** on cancer cells and to design and synthesize a few analogs of peptide **1** with enhanced bioactivity. Therefore, we designed two analogs of the lead peptide **1** (the linear peptide **2** and the cyclic peptide **3**) by addition of the RGD (Arg-Gly-Asp) sequence which serves as a cell adhesive carrier and provides a template for a better drug delivery and for inducing apoptosis of cancer cells [19]. The RGD-sequence is a

common cell-recognized motif, it presents in many extracellular matrix components such as fibronectin and vitronectin and it binds to integrins. RGD-containing peptides has been shown to influence caspase-3 and the downstream process of apoptosis. This sequence not only has been used as a leading compound for developing different integrin antagonists [20], but also used in the tumor targeting [21] and chemotherapeutic drugs [22]. The studies demonstrated that used fluorescence-activated cell-sorting (FACS) analysis to show targeted binding of the Arg-Gly-Asp (RGD)-peptide labeled with FITC, not only to endothelial cells but also to tumor cells in human breast cancer xenografts grown in nude mice. Nontumorous cells showed only background binding. And they suggested, that the RGD-peptide can target tumor endothelial cells as well as tumor cells. Consequently, it should be possible to design a combination therapy approach against both targets.

Binding affinity of peptides for Grb2 SH2 was analyzed by using the surface plasmon resonance technology developed with the Biosensor-BIAcore 2000. Effects of synthetic peptides on MCF-7 and MDA-MB-453 breast cancer cells were evaluated. The cell viability and cytotoxicity of peptide-treated cells were determined by using the cell proliferation kit (3-[4, 5-dimethyl-2-thiazolyl]-2, 5-diphenyl-tetrazolium bromide, MTT) and cytotoxicity kit (lactate dehydrogenase, LDH), respectively. Effects of peptides on the cell cycle progression of cancer cells and apoptosis were analyzed by using flow cytometry. Results of these studies provide important information for the development of anti-cancer agents.

Materials and methods

Design and synthesis of linear peptides

The structure-activity relationships of small peptidic inhibitors of Grb2 SH2 have been reported [18]. Among the synthetic peptidic inhibitors, the peptide **1** (Fmoc-Glu-Tyr-Aib-Asn-NH_2) with high affinity for Grb2 SH2 was selected as our lead peptide. A few peptide analogs of **1** were designed and synthesized (Figure 1-1). Their binding affinity for the Grb2 SH2 was assayed by surface plasmon resonance technology and their effects on breast cancer cells were investigated by *in vitro* bioassays.

(1)

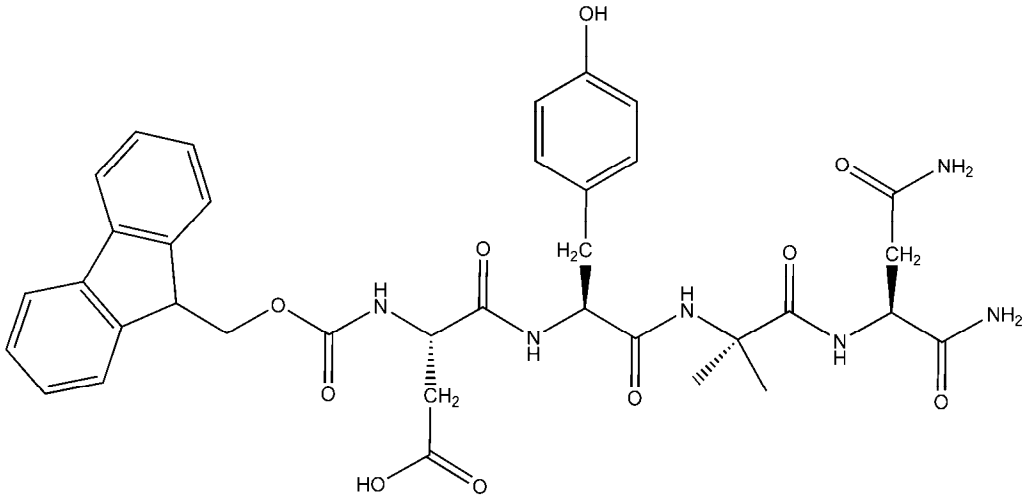

(2)

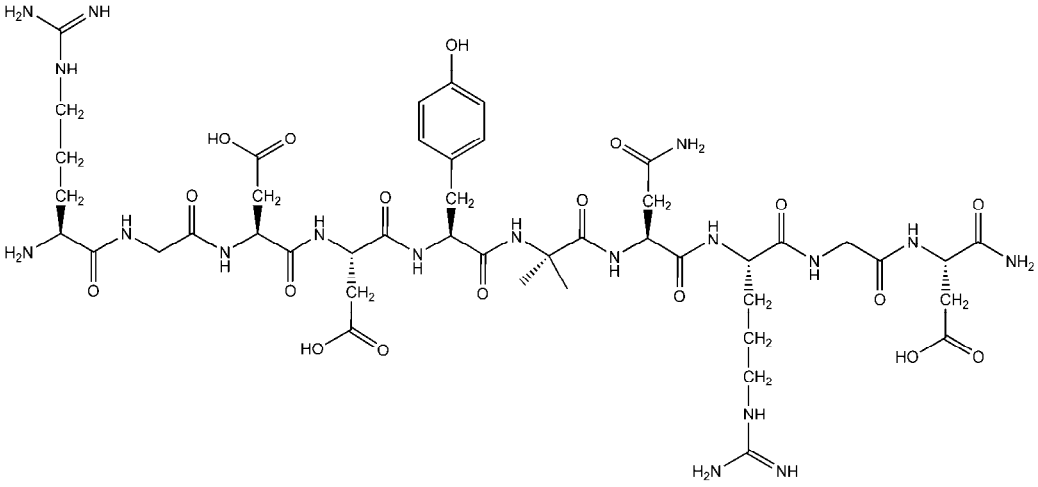

(3)

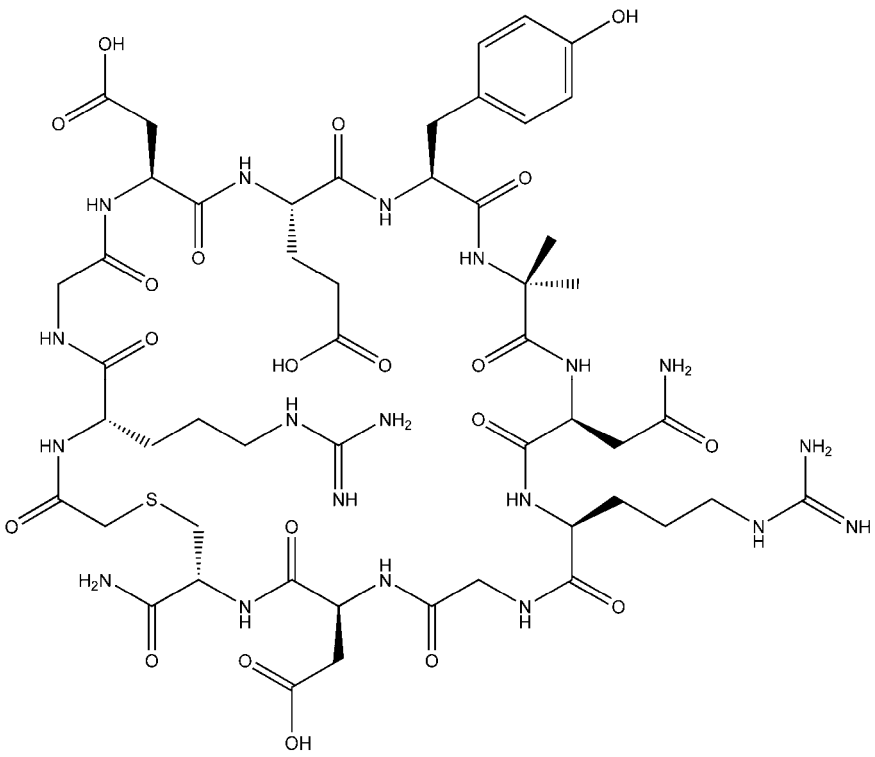

(4)

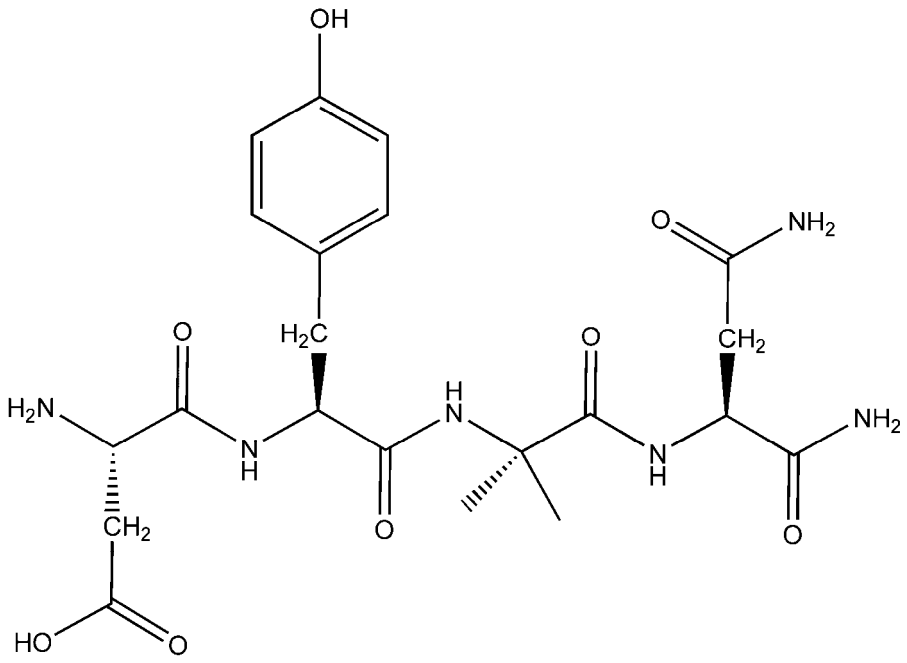

Figure 1-1. Chemical structures of designed peptides. (1) The structure of peptide **1**, Fmoc-Glu-Tyr-Aib-Asn-NH_2. (2) The structure of peptide **2**, H-Arg-Gly-Asp-Glu-Tyr-Aib-Asn-Arg-Gly-Asp-NH_2. (3) The structure of peptide **3**, Cyclic [Arg-Gly-Asp-Glu-Tyr-Aib-Asn-Arg-Gly-Asp-Cys]-NH_2. (4) The structure of peptide **4**, H-Glu-Tyr-Aib-Asn-NH_2.

Peptide analogs of **1** were synthesized manually **[**16**]** in our laboratory by solid phase peptide synthesis (SPPS) **[**23**]**, using Fmoc/tBu chemistry. Briefly, the Rink amide AM resin, 4-(2',4'-Dimethoxyphenyl)-Fmoc-aminomethyl-phenoxy-acetamido-norleucylaminomethyl resin, was swelled in DMF for 10 min at room temperature, followed by the removal of the Fmoc-protecting group on the resin by treatment with 20% piperidine in DMF for 15 min, repeated twice. The Nα-Fmoc, side-chain-protected amino acid, Fmoc–Asn(Trt)–OH, was activated by mixing with the coupling reagent, 1-hydroxybenzotriazole/ 2-(1H-benzotriazoleiyl)-tetramethyluronium hexafluorophosphate / N, N-diisopropylethylamine (HOBt/HBTU/DIEA, 1:1:2), for 5 min and then added to the reaction vessel for coupling with resin at room temperature for 1.5 hr. Cycles of deprotection of Fmoc and coupling with the subsequent amino acids were repeated to synthesize the desired peptide-bound resin. The crude peptide was removed from resin by TFA cleavage, lyophilized, and then purified by RP-HPLC on C18 column. After purification, the peptides were characterized by MALDI-TOF-MS spectrometry and RP-HPLC.

Synthesis of the cyclic peptide

Cycles of deprotection of Fmoc and coupling with the subsequent amino acids were repeated until the desired peptide-bound resin was completed. Then, the Fmoc-protecting group on the peptide-bound resin was removed by treatment with 20% piperidine in DMF for 15 min, repeated twice. Chloroacetic anhydride (4 equiv. in DMF) was added to the reaction vessel for chloroacetylation of the peptide-bound resin at room temperature overnight. The chloroacetylated linear peptide was simultaneously deprotected and cleaved from the resin using 95% TFA for 2 hr at room temperature. The filtrated from the TFA cleavage solution was evaporated by a gentle stream of N_2

gas. The crude chloroacetylated peptide was purified by RP-HPLC. For cyclization, the chloroacetylated peptide was added dropwisely into 50 mL of D.I. water by using a syringe pump, the pH value of the solution was adjusted at 8.5-9.0 by the addition of triethylamine, and the solution was kept stirring for 6-12 hr at room temperature. The crude cyclic peptide was lyophilized and purified, then, the purified cyclic peptide was characterized by MALDI-TOF-MS and RP-HPLC.

Biomolecular interaction analysis using SPR-biosensor

The GST-Grb2 SH2 was generated as reported previously [24]. Interactions of peptides **1** and **4** were analyzed and their dissociation equilibrium constant (K_D) were determined as reported recently [25]. Briefly, the surface of CM5 chip was activated by 0.1 M NHS/0.4M EDC (v/v = 1, 35 μL) at the flow rate of 5 μl/min. GST-Grb2 SH2 (30 μg/mL, 200 μL) were injected for immobilization on the sensor chip surface. Finally, 35 μL of ethanolamine hydrochloride (0.1 M, pH 8.5) was injected for blocking the activated surface. In this study, purified peptides **2** and **3** were diluted into various concentrations with HBS buffer, and each sample was introduced separately onto the GST-Grb2 SH2-immobilized CM5 chip at the flow rate of 25 μL/min for 3 min. The binding interaction between each peptide and the GST-Grb2 SH2 was detected and displayed as a sensorgram by plotting the RU (resonance unit) against time. Detected changes of RU represent the association and dissociation of GST-Grb2 SH2, and the data was analyzed using BIA evaluation software (Biacore AB, Pharmacia, Uppsala, Sweden) to determine the equilibrium constants of each peptide.

Cell culture

The breast cancer cell line MCF-7 (ErbB low-expression), and MDA-MB-453 (ErbB over-expression) were obtained from the Food Industry Research and Development Institute (Hsinchu, Taiwan). The cells were maintained in Dulbecco's modified Eagle's

Medium (DMEM) with 10% fetal bovine serum, 1% penicillin and streptomycin at 37 °C, 5% CO_2.

Determination of cell viability by using the cell proliferation assay

The proliferation of breast cells in the presence of various concentrations of peptides **1** and **2** were determined by using the MTT cell proliferation kit (Boehringer Manheim, Indianapolis, IN), following the manufacturer's protocol. Briefly, cells were plated in 24-well cell culture plates at a density of 1×10^6 cells/well in a final volume of 200 μL of medium and allowed to attach overnight. The cells were then treated with various concentrations of peptides **1** and **2** for 24, 48 and 72 hrs and treated with peptides **3** and **4** for 24 hrs. After completion of the treatment, the cells were incubated with MTT for 1 hr at 37 ^oC. Cells were lysed, and the reduced intracellular formazan product was dissolved in the buffer provided in the kit. MTT is reduced to formazan salt by live cells and quantified by an ELISA plate reader (Versamax, Sunnyvale, CA, USA) at 540 nm.

Determination of cell cytotoxicity by using the LDH assay

Lactate dehydrogenase leakage was measured to determine any acute membrane disturbance. The cytotoxicity of various concentrations of peptide **2** was determined using the LDH kit (Promega, USA). Briefly, 1×10^6 cells were plated in 24-well tissue culture plates overnight. The cells were then treated with varying doses of peptides **2** for 24, 48 and 72 hrs. After completion of the treatment, the supernatant of cell culture (50 μL medium/ well) was collected, followed by the addition of 50 μL of LDH solution and incubation for 30 min at room temperature. Lactate dehydrogenase leakage in the treated cells was quantified by an ELISA plate reader (Versamax, Sunnyvale, CA, USA) at 490 nm.

Flow cytometric analysis of DNA content and the cell cycle

Apoptotic cells were detected by FACS analysis of nuclear propidium iodide stained

cells. The cells (1 x 10^6 cells) were grown in 5 mL of DMEM containing 10% FBS for 24 hrs in the presence of various concentrations of the peptide **2**. For flow cytometry analysis, cells were trypsinized, pelleted by centrifugation, and fixed with 70% ethanol in PBS for 30 min at -20℃. After washing the cells with PBS, cells were permeabilized and stained with 500 μL of propidium iodide solution (50 μg/mL propidium iodide / 1% Triton X-100 / 0.1 mg/mL RNase in PBS) for 40 min at 37 ^{o}C, and then subjected to cell cycle analysis by using the Modifit cell cycle analysis software developed with a FACSCalibur Flow Cytometer (Becton Dickinson Immunocytometry Systems, Mountain View, CA).

Statistical Analysis

All values shown are means ± SEM (standard error of the mean). Differences between treated groups and controls were analyzed by one-way ANOVA followed by Dunnett's multiple comparison tests Differences in cell growth were analyzed by Student's t-test. Significance was accepted at $p < 0.05$.

Results

Design and synthesis of peptides

The Grb2 SH2 domain binds pTyr-containing motifs within several proteins including the adapter proteins SHC [26, 27], growth factor receptors such as members of the *erb*B family [27-30], morphology-determining proteins such as FAK [31], and cellular oncogenes such as BCR-*abl* [32, 33]. SH2 domain binding leads to activation of important downstream pathways by bringing the nucleotide exchange factor SOS1 to the membrane environment of p21*ras* [34]. A particularly important role for Grb2 in human cancer has been proposed for cells transformed by high levels of *erb*B2 (HER-2 or *neu*) expression [35]. In these cells, the SH2 domain of the Grb2 protein is primarily associated with pTyr residues on SHC and on erbB2 [36, 37].

A new small nonphosphorylated peptide, G1, that can selectively bind the Grb2 SH2 domain and block its function was identified by phage display (Figure 1-2) [37]. The alignment of the G1 sequence with Grb2 phosphopeptide ligands (Figure 1-2) suggests the importance of Tyr4 and Asn6 in G1. These residues have also previously been shown to be required for high affinity binding of pTyr-containing peptides to Grb2 SH2 domain [38].

Ala scanning within G1 and molecular modeling analysis suggest a promising model in which G1peptide binds in the phosphotyrosine binding site of the Grb2 SH2 domain in a β-turn-like conformation [39]. Replacement of Tyr4 or Asn6 with Ala abrogates the inhibitory activity of the peptide, indicating that G1 requires a Y-X-N consensus sequence similar to that found in natural pTyr-containing ligands. The Ala mutant of Glu2 remarkably reduces the binding affinity, and the molecular modeling results suggest that the side-chain of Glu2 provide a complementary role for pTyr.

G1 (disulfide bridged peptide)	C-E-L- Y-E-N-V-G-M-Y-C
SHC (pY317)	F-D-D-P-S-pY-V-N-V-Q
EGF receptor (pY1068)	L-P-V-P-E-pY- I-N-Q-S-V
EGF receptor (pY1138)	V-G-N-P-E-pY-L-N-T-V-Q
Concensus sequence:	
pY-ligand to Grb2 SH2	P-X-pY-X-N
non-pY to Grb2 SH2	E-L- Y -E-N

Figure 1-2. Sequence of the G1 peptide in comparison with known Grb2 binding phosphopeptide sequences.

On the basis of results of structure activity relationships of G1 peptide and Novartist's compounds [40] , peptide analogs with the sequence of Fmoc-X_1-Tyr-X_2-Asn (X_1 = Glu, Adi, or Gla, X_2 = Aib or Ach) were designed, synthesized, and assayed for their binding potency with Grb2 SH2 [18]. Since Grb2 SH2 recognizes a β-hairpin motif and binds phosphotyrosyl peptides with the consensus sequence pYXNX [41, 42], we incorporated α-aminoisobutyric acid (Aib) into peptide **1** in order to stabilize a folded structure [43], increase conformational rigidity of the peptides, or enhance their binding affinity for Grb2 SH2. In Novartist's compounds, the 3-aminobenzyloxycarbonyl group at pY-1 position caused a dramatic increase of the binding affinity of phosphopeptides for Grb2 SH2 [39], therefore, we kept the Fmoc group at the N-terminal of the peptide **1** in order to mimic the 3-aminobenzyloxycarbonyl group incorporated in the potent phosphopeptide inhibitors, while the peptide **4** was designed to demonstrate the important effect of the N-terminal functional group on the binding affinity for Grb2 SH2.

The RGD motif is not only used extensively as inhibitor of integrin-ligand but also used to develop the potential inhibitor of signal transduction pathway for cancer therapy. RGD-containing peptides are capable of inducing cell apoptosis [19]. Therefore, in this study, the linear peptide analog **2** and cyclic peptide analog **3** (Figure 1-1) were designed by addition of the RGD motif to both the N- and C-terminal of peptide **4** in order to enhance the potency of peptide analogs. Cyclic peptide **3** was designed in order to increase the stability of peptide and to examine the effect of rigidity on the binding affinity for Grb2 SH2.

Synthesized peptides were purified and characterized by RP-HPLC and MALDI-TOF mass spectrometry (Table 1-1)

Table 1-1. Physicochemical characterization of designed peptides

Peptide	Sequence	RP-HPLC (Rt, min)	Purity (%)	MALDI-TOF (Daltons)
1[a]	Fmoc-Glu-Tyr-Aib-Asn-NH_2	15.12	95	730.74
2	H-Arg-Gly-Asp-Glu-Tyr-Aib-Asn-Arg-Gly-Asp-NH_2	5.52	94	1165.17
3	Cyclic[Arg-Gly-Asp-Glu-Tyr-Aib-Asn-Arg-Gly-Asp-Cys]-NH_2	6.67	96	1308.33
4[a]	H-Glu-Tyr-Aib-Asn-NH_2	15.42	95	507.49
5	H-Arg-Gly-Asp-NH_2	11.72	96	347.18

[a]Peptides 1 and 4 were reported in Protein and Peptide Letters, 2008, 15, 806-810.

Detection of interactions between the immobilized GST-Grb2 SH2 and peptide

The surface plasmon resonance (SPR) technology [44] has been applied extensively to study various biomolecular interactions. Previously, this technology was applied to investigate the inhibitory effects of synthetic peptide inhibitors on the interactions between GST-Grb2 SH2 and its binding ligand, the Shc phosphopeptide, by using BIACORE 2000 instrument [37]. We also used the semi-automatic BIACORE X instrument to establish the SPR-based assays for determining the inhibitory potency of peptides [16]. Briefly, the biotin-Shc phosphopeptide was immobilized on flow cells 2 (Fc2) of the surface of sensor chip SA. Inhibitory effects of the free Shc(pY) and synthetic peptides on the interactions between Grb2 SH2 and the immobilized Shc(pY) were investigated by a competitive binding assay. Recently, we reported the application of the GST-Grb2 SH2-immobilized assay to determine the equilibrium dissociation constants (K_D) for peptides **1** and **4** (6.3×10^{-9} M and 3.1×10^{-5} M, respectively) [25]. In this study, the equilibrium dissociation constants (K_D) of peptides **2** and **3** were determined as 1.2×10^{-8} and 4.1×10^{-6}, respectively, by using the same assay (Table 1-2). Briefly, binding interactions between various concentrations of peptide and GST-Grb2 SH2 were detected and displayed as sensorgrams (data not shown). Detected RU changes represent the association and dissociation of GST-Grb2 SH2, and the data collected for each peptide was analyzed using BIA evaluation software.

Table 1-2. Equilibrium dissociation constants of synthetic peptides

Peptide	K_D[a] (M)
1[b]	6.3×10^{-9}
2	1.2×10^{-8}
3	4.1×10^{-6}
4[b]	3.1×10^{-5}

[a] K_D : equilibrium dissociation constant

[b] the K_D value of peptides **1** and **4** were reported in Protein and Peptide Letters, 2008, 15, 806-810.

The binding potency of peptide **4** to Grb2 SH2 was reduced significantly due to the removal of Fmoc group from peptide **1**, however, peptide **2** (with the addition of RGD on both N- and C-terminal of the lead peptide **1)** and peptide **3** (by cyclization of peptide **2**) greatly enhanced the binding potency of peptide **4** to Grb2 SH2 by these modifications.

Antiproliferative effects of peptides in breast cancer cells

Previously, the inhibitory effects of synthetic peptides on the interactions between Grb2 SH2 and the immobilized Shc(pY) was assessed by the competitive binding assay, and the SPR-derived IC_{50} values provide an indication of the ability of peptides to bind to isolated Grb2 SH2 protein *in vitro*. However, this measurement may not reflect their biological effects in the intact cells, because peptide inhibitors must cross cell membranes in order to interact with the target proteins. Therefore, it is necessary to perform the cell proliferation assays with synthetic peptides to measure their antiproliferative effects in MCF-7 and MDA-MB-453 breast cancer cells. MDA-MB-453 breast cancer cells [45] with overexpressed erbB-2 are mitogenically driven through Grb2-dependent signaling pathways. In contrast, MCF-7 breast cancer cells [46] have a low-expression of erbB-2 as compared with MDA-MB-453 cells.

Peptides **1** exhibited antiproliferative effects in MCF-7 and MDA-MB-453 cancer cells at 25, 50, 75 and 100 μM (Figures 1-3a and 1-3b). By treatment of MCF-7 and MDA-MB-453 with 75 μM of peptide **1** for 24 hrs, the inhibitory effects in MCF-7 and MDA-MB-453 cells were detected as 15% and 35% inhibition of cell proliferation, respectively (Figures 3a and 3b)

(a)

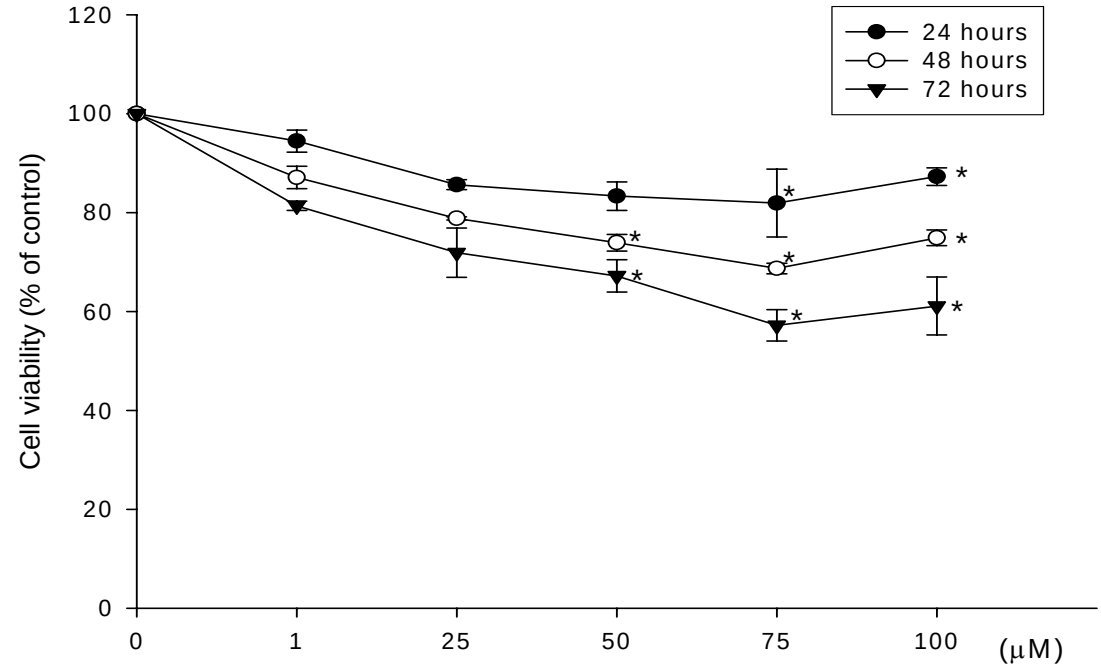

(b)

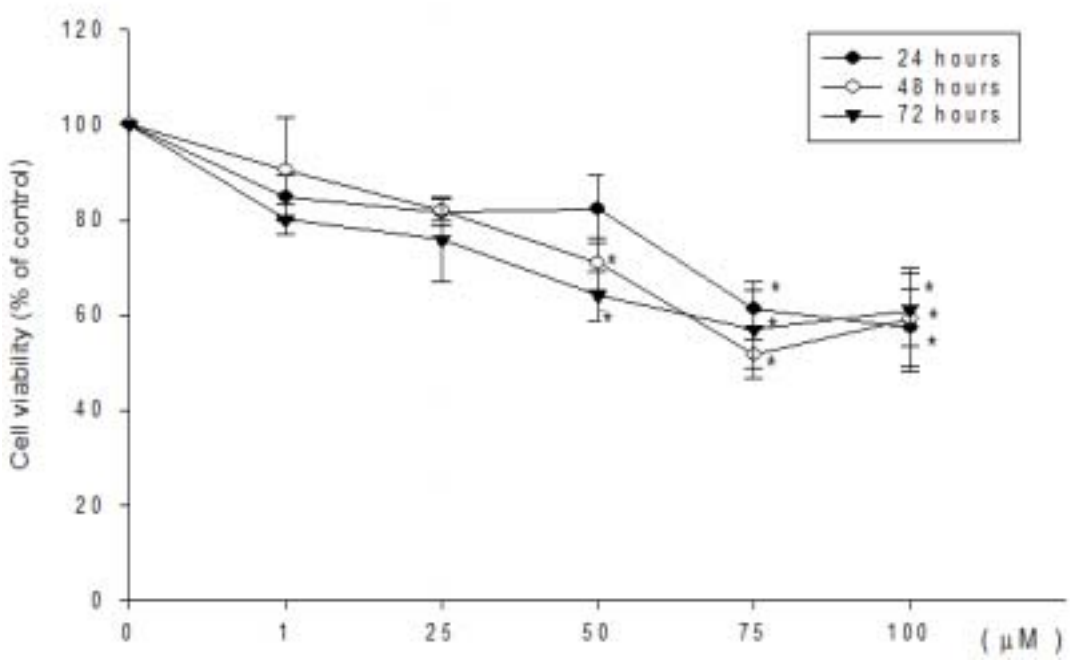

Figure 1-3. Time and dose-dependent curves for peptide **1** in the MTT reduction assay. Human breast cancer cells MCF-7(a), MDA-MB-453(b) were treated with 0, 1, 25, 50, 75 and 100 μM of peptide **1** for 24, 48 and 72 hrs. The data shown represent the mean ± SEM of the mean cell counts from three independent experiments performed and analyzed as described.

Peptides **2** exhibited significant antiproliferative effects in MCF-7 and MDA-MB-453 cancer cells at 25, 50, 75 and 100 μM. (Figure 1-4a and Figure 1-4b). By treatment of MCF-7 and MDA-MB-453 with 75 μM of peptide **2** for 24 hrs, the inhibitory effects in MCF-7 and MDA-MB-453 cells were detected as 40% and 40% inhibition of cell proliferation, respectively (Figures 1-4a and 1-4b).

By treatment of both cancer cells with 75 μM of **3** for 24 hrs, cyclic peptide **3** caused only 26% and 24% inhibition of the proliferation of MCF-7 and MDA-MB-453 cancer cells, respectively (Figures 1-5a and 1-5b). These results demonstrated that peptide **2** exhibited the greatest inhibitory effects on cell proliferation in both cancer cells among peptides **1** - **3,** indicating the incorporation of RGD into peptide enhance the inhibitory effect, while the cyclization of RGD-containing peptide reduced the inhibitory effect on the proliferation of cancer cells.

By treatment of both cancer cells with 75 μM of peptide **4** for 24 hrs, peptide **4** did not show significant inhibition of the proliferation of MCF-7 and MDA-MB-453 cancer cells, respectively (Figures 1-6a and 1-6b), indicating the removal of Fmoc group from peptide **1** reduced the inhibitory effect on the proliferation of cancer cells.

The half maximal inhibitory concentrations (IC_{50}) values of peptides **1** and **2** were determined by treatment of MCF-7 and MDA-MB-453 cancer cells with each peptide for 72 hrs. The IC_{50} of peptide **1** in both cancer cells were greater than 100 μM (Figure 1-7a), while the IC_{50} of peptide **2** determined in MCF-7 and MDA-MB-453 cancer cells were 45.7 μM and 47.4 μM, respectively (Figure 1-7b).

(a)

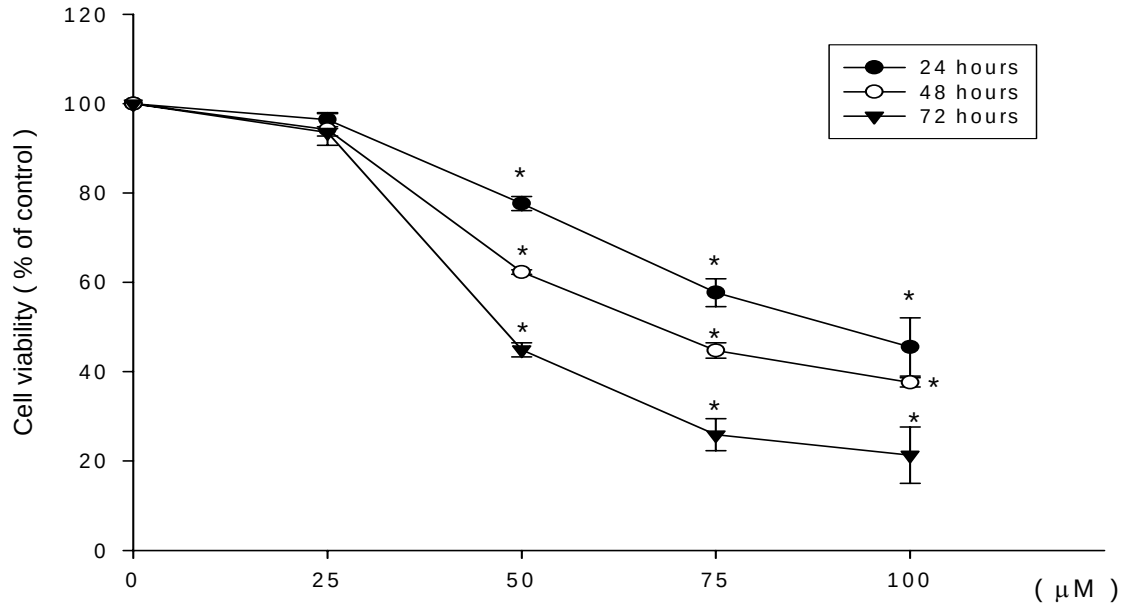

(b)

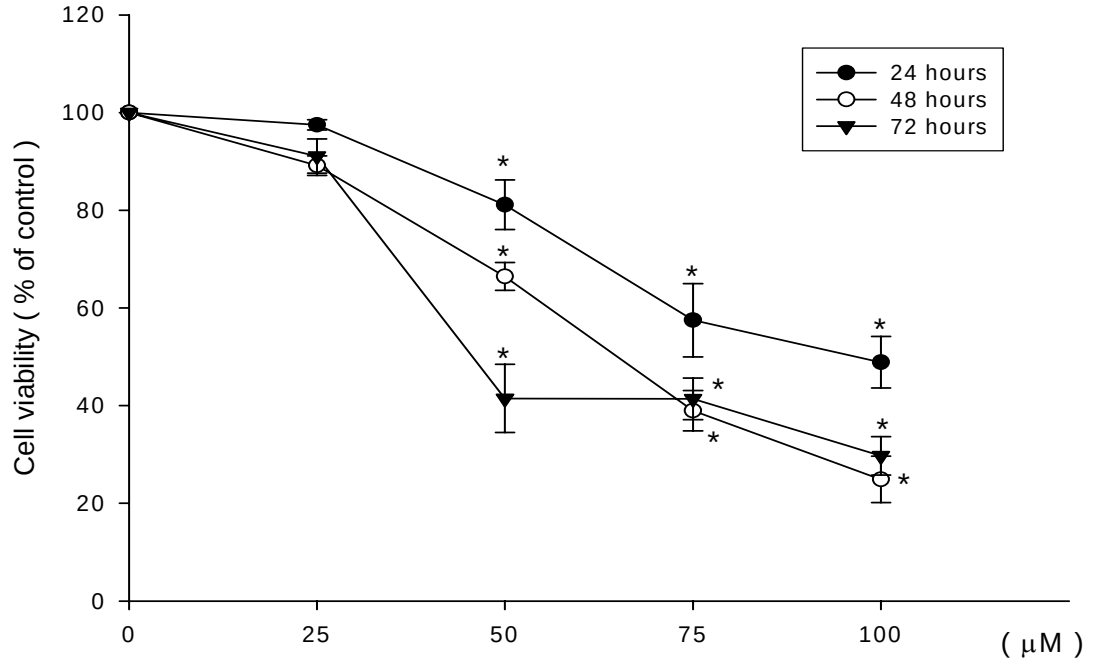

Figure 1-4. Time and dose-dependent curves for peptide **2** in the MTT reduction assay. Human breast cancer cells MCF-7(a), MDA-MB-453(b) were treated with 0, 25, 50, 75, and 100 μM of peptide **2** for 24, 48 and 72 hrs. The data shown represent the mean ± SEM of the mean cell counts from three independent experiments performed and analyzed as described.

(a)

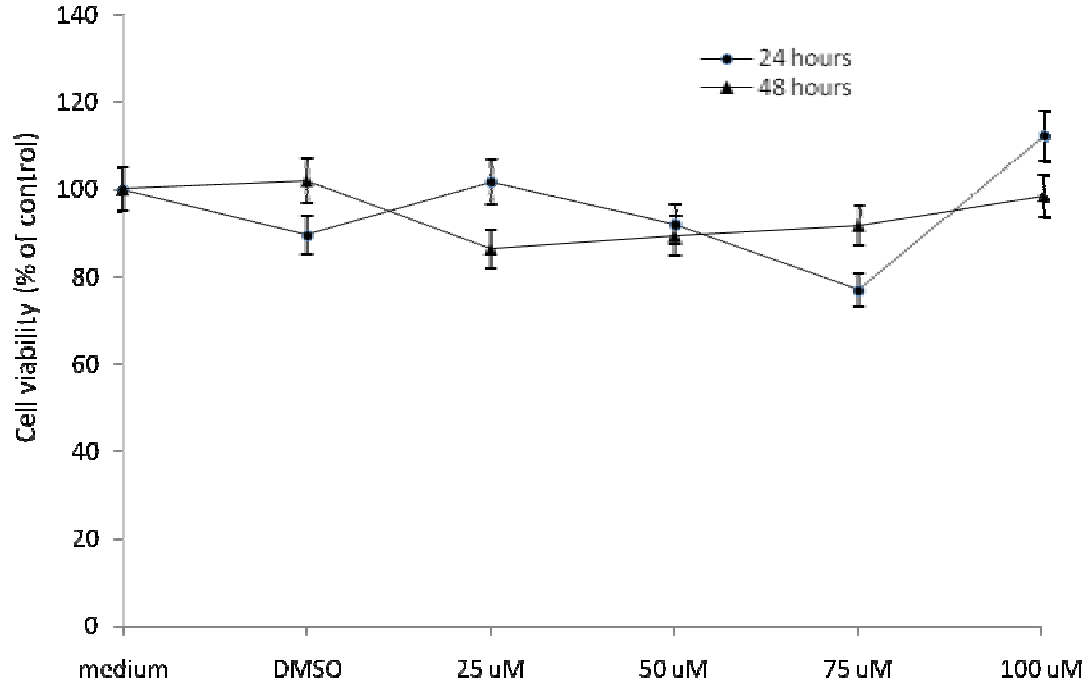

(b)

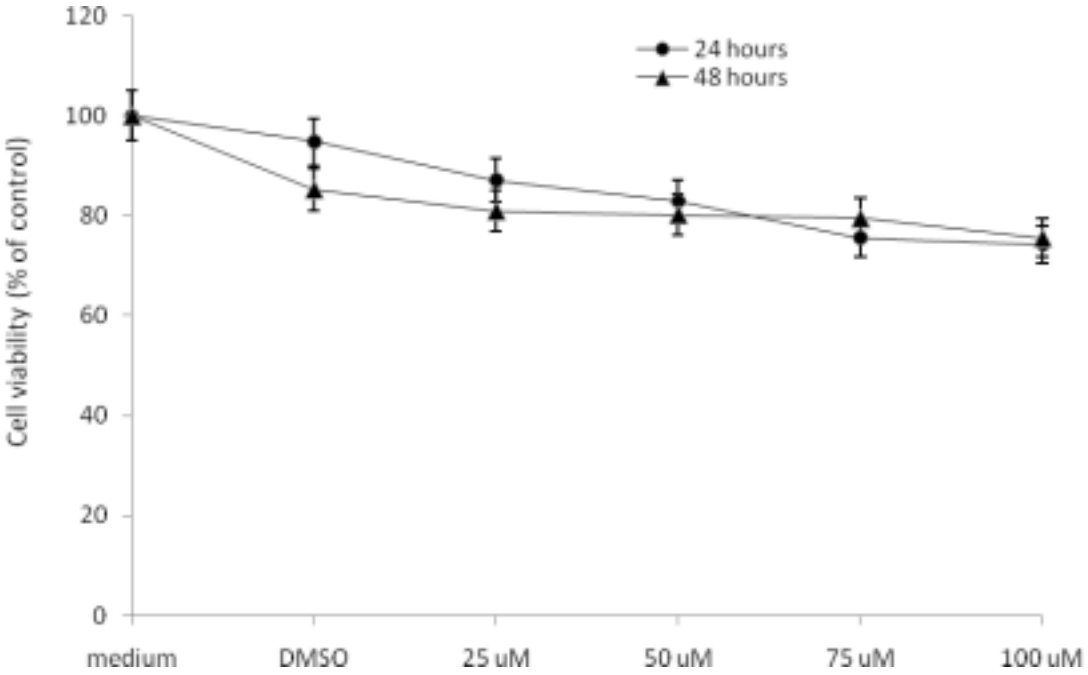

Figure 1-5. Time and dose-dependent curves for peptide **3** in the MTT reduction assay. Human breast cancer cells MCF-7(a), MDA-MB-453(b) were treated with 0, 25, 50, 75 and 100 μM of peptide **3** for 24 and 48 hrs. The data shown represent the mean ± SEM of the mean cell counts from three independent experiments performed and analyzed as described.

(a)

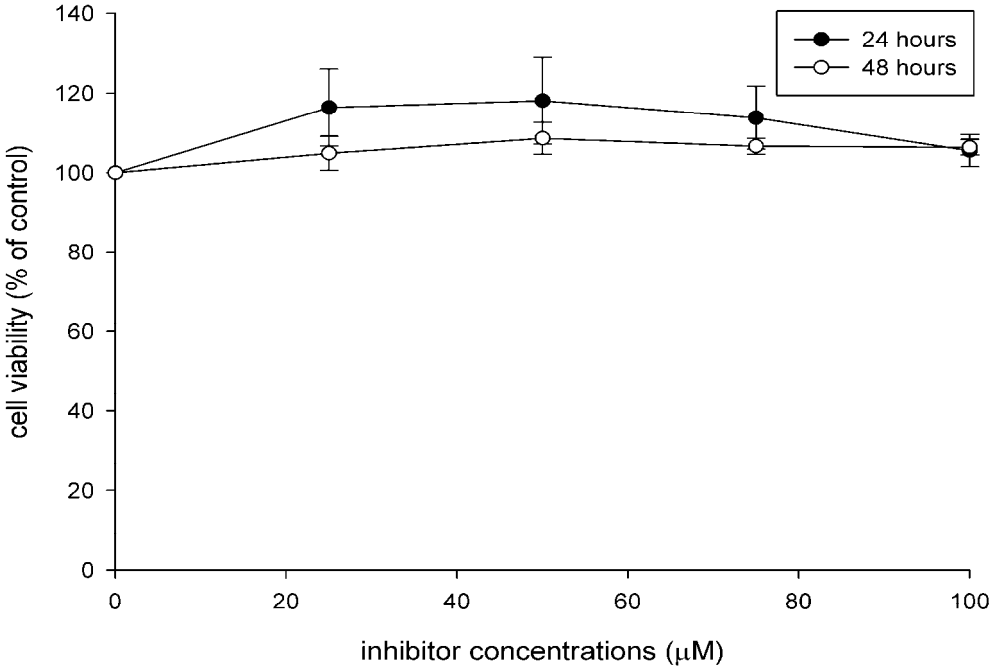

(b)

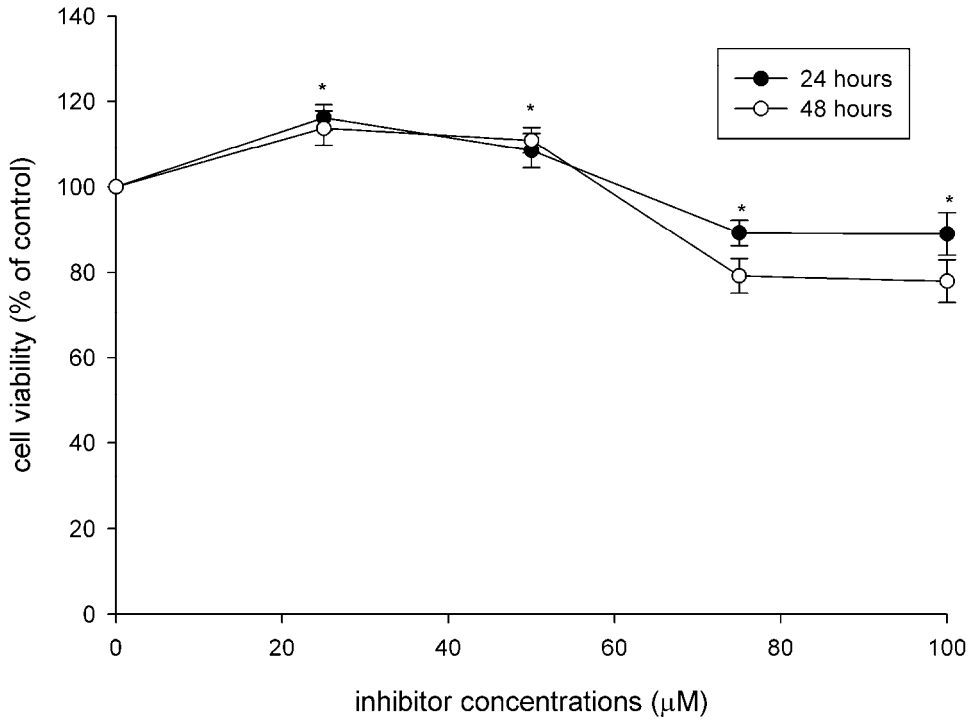

Figure 1-6. Time and dose-dependent curves for peptide **4** in the MTT reduction assay. Human breast cancer cells MCF-7(a), MDA-MB-453(b) were treated with 0, 25, 50, 75, and 100 μM of peptide **4** for 24 hrs and 48 hrs. The data shown represent the mean ± SEM of the mean cell counts from three independent experiments performed and analyzed as described.

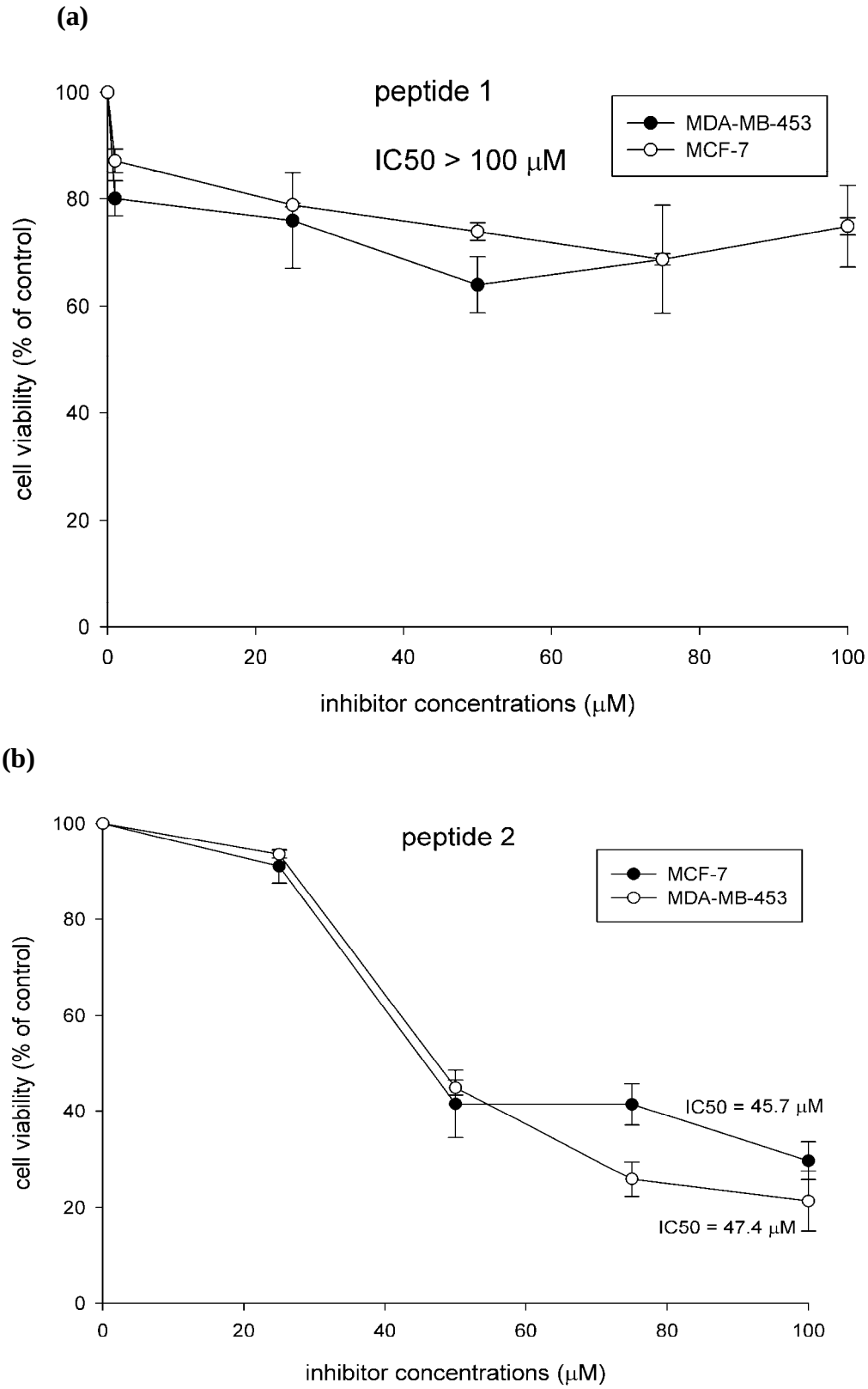

Figure 1-7. IC_{50} plotting. Effects of peptides on the cell viability was determined as the IC_{50} value of peptide after 72 hrs-treatment of indicated breast cancer cells with various concentrations of peptide **1** (a), peptide **2** (b)

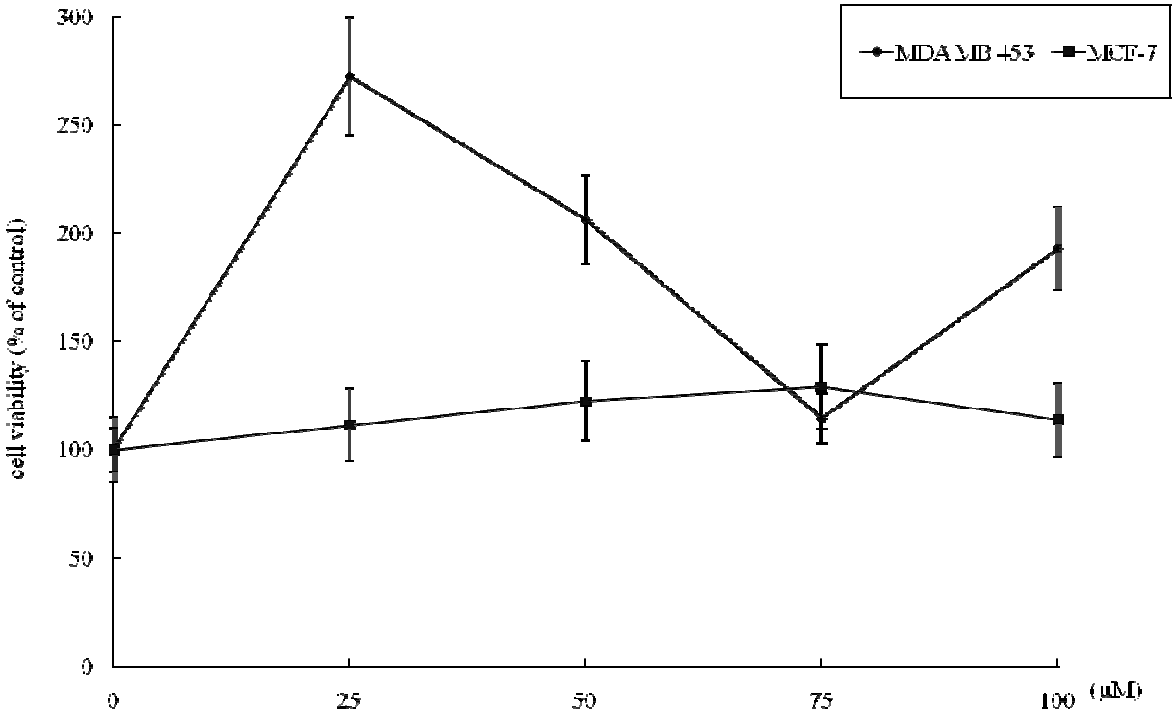

Figure 1-8. Time and dose-dependent curves for RGD in the MTT reduction assay. Human breast cancer cells MCF-7 and MDA-MB-453 were treated with RGD tripeptide for 24 hrs. The data shown represent the mean ± SEM of the mean cell counts from three independent experiments performed and analyzed as described.

Since the peptide synthesized is being developed as a potential treatment for cancer, its specificity for these cells is important, and the effect of peptide **2** on non-cancer cells needs to be tested. Thus, the effect of peptide **2** on non-cancer cells, human skin cells (HS-68), was also tested. Peptides **2** did not exhibited significant antiproliferative effects on human skin cells, HS-68, at 25, 50, 75 and 100 μM. (Figure 1-9). Even by treatment of HS-68 with 100 μM of peptide **2** for 24 and 48 hrs, the inhibitory effect of peptide **2** on HS-68 cells were not detected, indicating our designed peptide exhibited the specificity for cancer cells.

Cytotoxicity effect in breast cancer cells

Effects of the peptide 2 on the membrane integrity and cellular toxicity of the MDA-MB-453 and MCF-7 were determined by LDH release assay. The LDH release of the peptide **2**-treated breast cancer cells was in a dose-dependent manner (Figure 1-10), indicating peptide 2 exhibited cytotoxicity effect in the breast cancer cells.

Effects of synthetic peptides on the cell cycle

Cells were treated with peptide **2** (25 to 100 μM). After 24 hrs of culture, cells were harvested and their DNA content was analyzed by flow cytometry. The peptide **2**-treated MCF-7 and MDA-MB-453 cells showed a decreased G0/G1 phase and an increased sub-G1 peak in the cell cycle (Figure 1-11), indicating the induction of apoptosis of cancer cells by the treatment of cancer cells with 100 μM of peptide **2** for 24 hrs. This result is in agreement with the MTT result, indicating the antipeliferative effect of peptide **2** on breast cancer cells was correlated with its induction of apoptosis.

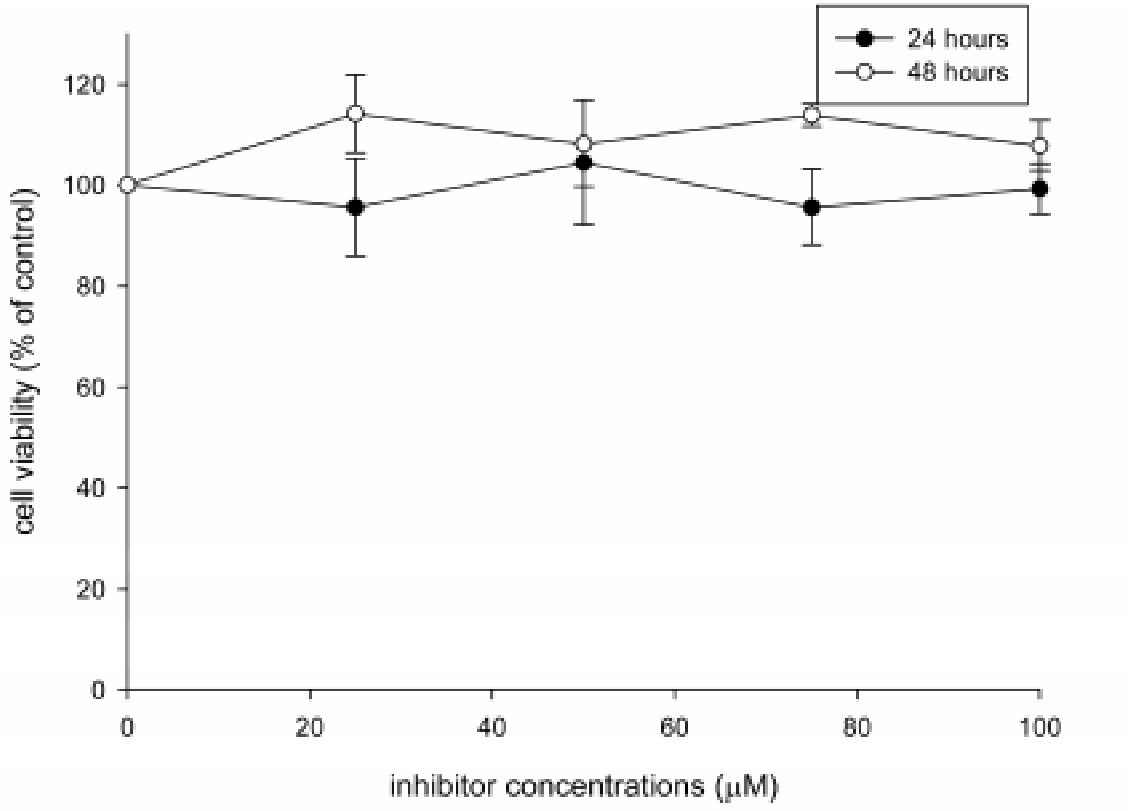

Figure 1-9. Time and dose-dependent curves for peptide **2** in the MTT reduction assay. Human skin cells HS-68 were treated with 0, 25, 50, 75 and 100 μM of peptide **2** for 24 and 48 hrs. The data shown represent the mean ± SEM of the mean cell counts from three independent experiments performed and analyzed as described.

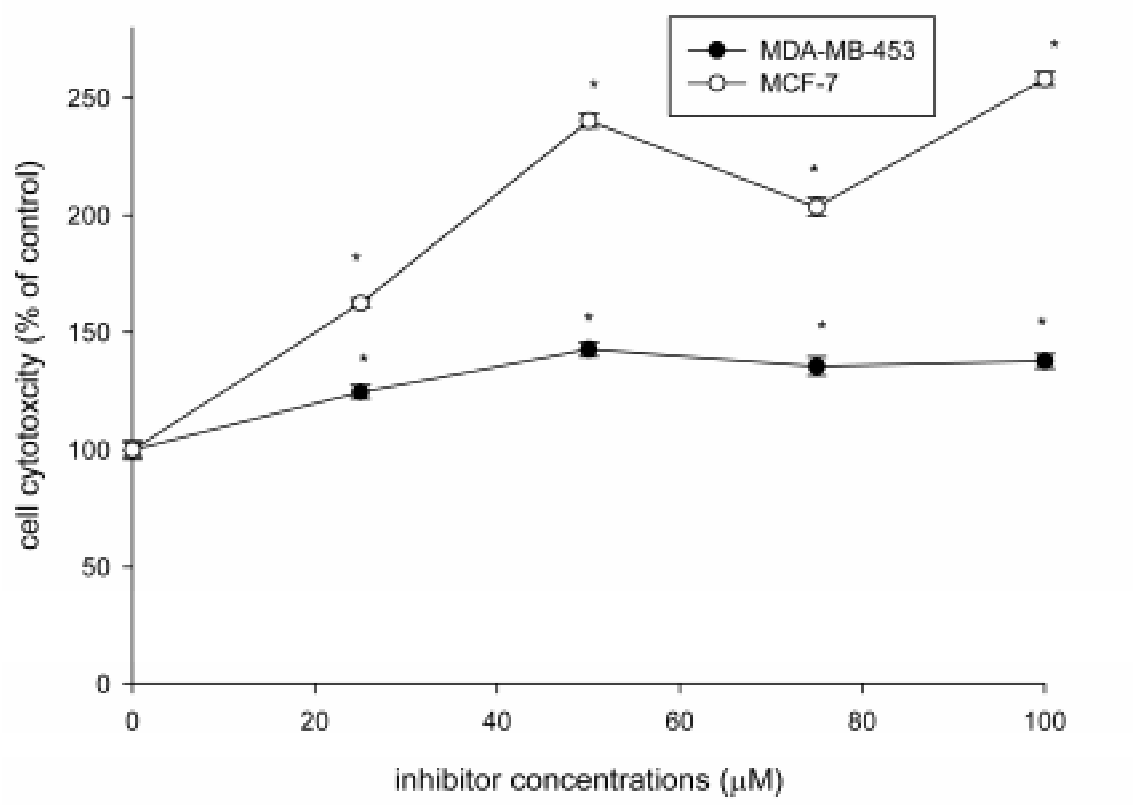

Figure 1-10. Dose-response curve of cytotoxicity was determined by the LDH assay of peptide **2**-treated breast cancer cells.

* Significant different at $p < 0.05$ level as compared with medium control. Data are presented as the mean ± SD (n＝3)

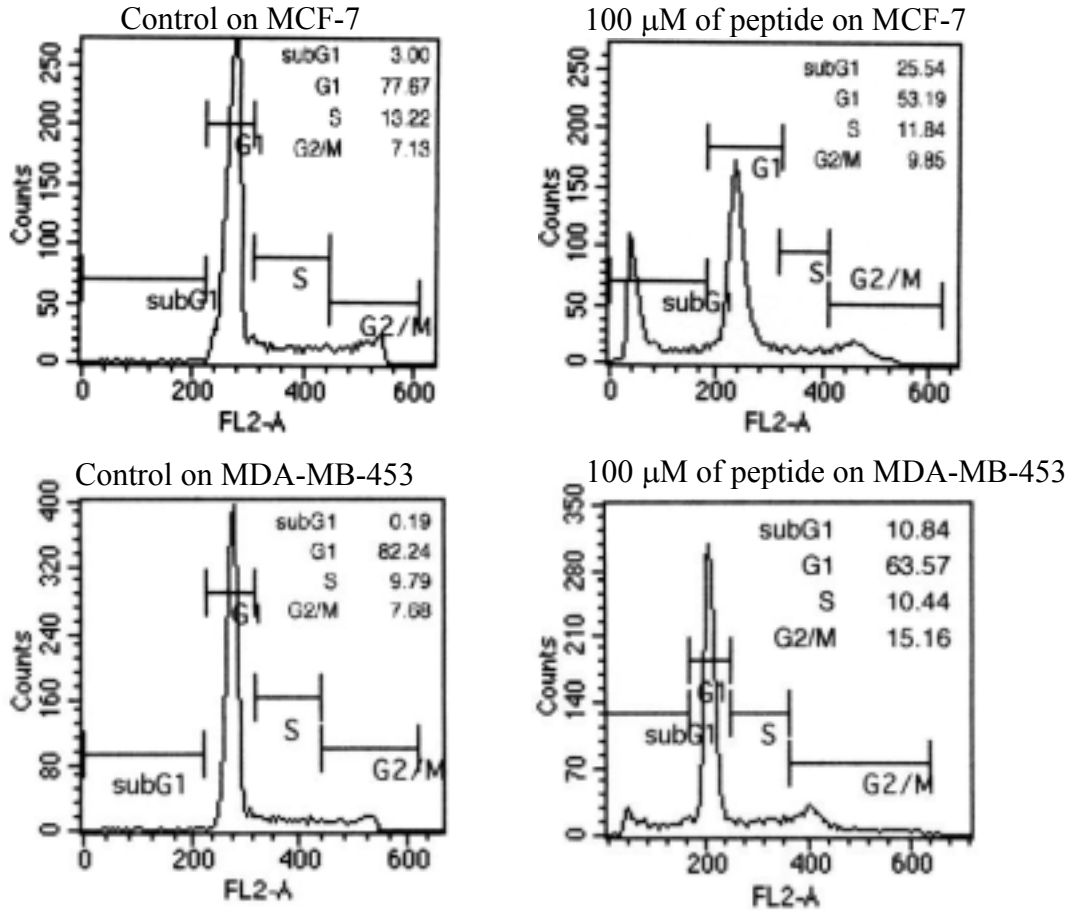

Figure 1-11. Effects of peptide **2** on cell cycle of breast cancer cell lines. The cells were incubated with 100 μM of peptide **2** for 24 hrs, and they were harvested and analyzed by flow cytometry.

Discussion

In this study, the linear peptide analog **2** and cyclic peptide analog **3** (Figure 1-1) were designed by addition of the RGD motif to both the N- and C-terminal of peptide **4** in order to enhance the potency of peptide analogs. Because of the RGD motif is not only used extensively as inhibitor of integrin-ligand but also used to develop the potential inhibitor of signal transduction pathway for cancer therapy. RGD-containing peptides are capable of inducing cell apoptosis [19]. In order to increase the stability of peptide, therefore, Cyclic peptide **3** was designed and to examine the effect of rigidity on the binding affinity for Grb2 SH2.

The equilibrium constants of peptide analogs of the leading peptide discovered by SPR technology were determined. Peptides with affinity for the Grb2 SH2 were further assayed for their effects on breast cancer cells. Though the incorporation of RGD motif into the lead peptide dose not enhance the effect on binding to the Grb2 SH2 domain (K_D for **2** vs. **1**, 1.2×10^{-8} M vs. 6.3×10^{-9} M). As shown in Figures 3-6, treatment of MCF-7 cancer cells with 75 μM of peptides **1**-**4** for 24 hrs, the inhibition of cell proliferation were 15%, 40%, 26%, and 0, respectively, while treatment of MDA-MB-453 cancer cells with 75 μM of peptides **1**-**4** for 24 hrs, the inhibition of cell proliferation were 35%, 40%, 24%, and 15%, respectively. Results demonstrated that the peptide **2** exhibited the strongest inhibitory effect and the peptide **4** showed the least inhibitory effect on the proliferation of both cancer cells. SPR results demonstrated that the binding affinity of peptide **4** for Grb2 SH2 was significantly reduced because the removal of the Fmoc group, while the binding potency of both peptides **2** and **3**, which have the additional Arg-Gly-Asp sequence on both the N- and C-terminal of peptide **4**, was greater than that of peptide **4**. These results explain why peptides **2** and **3** are more effective on inhibiting the proliferation of cancer cells than peptide **4**. Though the addition of RGD on both terminals of peptide **1** and the cyclization of RGD-containing

peptide did not enhance the binding affinity of peptide **1** for the Grb2 SH2 domain, these modifications affected the bioactivity of peptides in cancer cells. The linear compound **2** is a significant improvement from the lead compound, whereas the cyclic analog is much less active.

Although peptide **2** is more effective on cancer cells compared to peptide **1** (which lacks Arg-Gly-Asp), it is important to clarify if the action of peptide **2** due solely to the Arg-Gly-Asp or the rest Glu-Tyr-Aib-Asn sequence in peptide **2** is still needed. In order to rule out the possibility that an H-Arg-Gly-Asp-NH_2 tri-peptide will give the same result as peptide **2**, we synthesized the tri-peptide as the control, and investigated its effect on the proliferation of cancer cells by performing the MTT assay. We found that the tri-peptide did not inhibit the proliferation of cancer cells (Figure 1-8), indicating that the Glu-Tyr-Aib-Asn sequence in peptide **2** is important for inhibition of the proliferation of cancer cells. The bioactivity was enhanced dramatically (the IC_{50} of 72 h-treatment of **2** in MCF-7 and MDA-MB-453 cancer cells were 45.7 μM and 47.4 μM, while the IC_{50} of 72 hrs-treatment of **1** in MCF-7 and MDA-MB-453 cancer cells were greater than 100 μM).

Peptide **2** induced typical apoptotic characteristics in MCF-7 and MDA-MB-453 cells such as cell shrinkage, chromatin condensation, plasma membrane blebbing, oligonucleosomal DNA fragmentation and finally breakdown of the cells into smaller units.

Grb2 SH2 has been a potential target for cancer therapy because of its involvement in the oncogenic Ras signaling pathway. Herein, we report the further design of a lead peptide, Fmoc-Glu-Tyr-Aib-Asn-NH_2, by addition of an Arg-Gly-Asp sequence to the lead peptide to enhance binding to Grb2 SH2 and inducing apoptosis in cancer cells. Both the linear and cyclic analogs of the newly designed compound were prepared along with an analog in which the N^{α}-Fmoc group was removed. These peptide

analogs were assayed for their affinity for the Grb2 SH2, their antiproliferative effect on breast cancer cells, their specificity for cancer cells, and their effects on cytotoxicity and the cell cycle. Though the addition of Arg-Gly-Asp motif to the lead peptide dose not enhance the affinity for the Grb2 SH2 domain, the bioactivity was enhanced dramatically (the IC_{50} of peptide **2** in MCF-7 and MDA-MB-453 were 45.7 μM and 47.4 μM, respectively, while the IC_{50} of peptide **1** in both MCF-7 and MDA-MB-453 were greater than 100 μM). The linear peptide **2** is a significant improvement from the lead compound and become the new leading peptide that is useful for further development of antiproliferative agents. The design feature of peptide **2** is interesting and could lead to a biologically useful compound.

References

1. Garbay, C.; Liu, W. Q.; Vidal, M.; Roques, B. P. Inhibitors of Ras signal transduction as antitumor agents. Biochem Pharmacol 2000; **60**: 1165-1169.
2. Pawson, T. Protein-tyrosine kinases. Getting down to specifics. Nature 1995; **373**: 477-478.
3. Shakespeare, W. C. SH2 domain inhibition: a problem solved? Curr Opin Chem Biol 2001; **5**: 409-415.
4. Silvennoinen, O.; Schindler, C.; Schlessinger, J.; Levy, D. E. Ras-independent growth factor signaling by transcription factor tyrosine phosphorylation. Science 1993; **261**: 1736-1739.
5. Cohen, G. B.; Ren, R.; Baltimore, D. Modular binding domains in signal transduction proteins. Cell 1995; **80**: 237-248.
6. Pawson, T.; Scott, J. D. Signaling through scaffold, anchoring, and adaptor proteins. Science 1997; **278**: 2075-2080.
7. Mayer, B. J.; Gupta, R. Functions of SH2 and SH3 domains. Curr Top Microbiol Immunol 1998; **228**: 1-22.
8. Wei, C. Q.; Li, B.; Guo, R.; Yang, D.; Burke, T. R., Jr. Development of a phosphatase-stable phosphotyrosyl mimetic suitably protected for the synthesis of high-affinity Grb2 SH2 domain-binding ligands. Bioorg Med Chem Lett 2002; **12**: 2781-2784.
9. Li, P.; Zhang, M.; Peach, M. L.; Zhang, X.; Liu, H.; Nicklaus, M.; Yang, D.; Roller, P. P. Structural basis for a non-phosphorus-containing cyclic peptide binding to Grb2-SH2 domain with high affinity. Biochem Biophys Res Commun 2003; **307**: 1038-1044.
10. Jiang, S.; Li, P.; Peach, M. L.; Bindu, L.; Worthy, K. W.; Fisher, R. J.; Burke, T. R., Jr.; Nicklaus, M.; Roller, P. P. Structure-based design of potent Grb2-SH2 domain antagonists not relying on phosphotyrosine mimics. Biochem Biophys Res Commun 2006; **349**: 497-503.
11. Song, Y. L.; Peach, M. L.; Roller, P. P.; Qiu, S.; Wang, S.; Long, Y. Q. Discovery of a novel nonphosphorylated pentapeptide motif displaying high affinity for Grb2-SH2 domain by the utilization of 3'-substituted tyrosine derivatives. J Med Chem 2006; **49**: 1585-1596.
12. Maignan, S.; Guilloteau, J. P.; Fromage, N.; Arnoux, B.; Becquart, J.; Ducruix, A. Crystal structure of the mammalian Grb2 adaptor. Science 1995; **268**: 291-293.
13. Lowenstein, E. J.; Daly, R. J.; Batzer, A. G.; Li, W.; Margolis, B.; Lammers, R.; Ullrich, A.; Skolnik, E. Y.; Bar-Sagi, D.; Schlessinger, J. The SH2 and SH3 domain-containing protein GRB2 links receptor tyrosine kinases to ras signaling. Cell 1992; **70**: 431-442.

14. Smithgall, T. E. SH2 and SH3 domains: potential targets for anti-cancer drug design. J Pharmacol Toxicol Methods 1995; **34**: 125-132.
15. Fretz, H.; Furet, P.; Garcia-Echeverria, C.; Schoepfer, J.; Rahuel, J. Structure-based design of compounds inhibiting Grb2-SH2 mediated protein-protein interactions in signal transduction pathways. Curr Pharm Des 2000; **6**: 1777-1796.
16. Lung, F. D.; Tsai, J. Y.; Wei, S. Y.; Cheng, J. W.; Chen, C.; Li, P.; Roller, P. P. Novel peptide inhibitors for Grb2 SH2 domain and their detection by surface plasmon resonance. J Pept Res 2002; **60**: 143-149.
17. Lung, F. D.; Tsai, J. Y. Grb2 SH2 domain-binding peptide analogs as potential anticancer agents. Biopolymers 2003; **71**: 132-140.
18. Lung, F. D.; Chang, C. W.; Chong, M. C.; Liou, C. C.; Li, P.; Peach, M. L.; Nicklaus, M. C.; Lou, B. S.; Roller, P. P. Small nonphosphorylated Grb2-SH2 domain antagonists evaluated by surface plasmon resonance technology. Biopolymers 2005; **80**: 628-635.
19. Buckley, C. D.; Pilling, D.; Henriquez, N. V.; Parsonage, G.; Threlfall, K.; Scheel-Toellner, D.; Simmons, D. L.; Akbar, A. N.; Lord, J. M.; Salmon, M. RGD peptides induce apoptosis by direct caspase-3 activation. Nature 1999; **397**: 534-539.
20. Sulyok, G. A.; Gibson, C.; Goodman, S. L.; Holzemann, G.; Wiesner, M.; Kessler, H. Solid-phase synthesis of a nonpeptide RGD mimetic library: new selective alphavbeta3 integrin antagonists. J Med Chem 2001; **44**: 1938-1950.
21. van Hagen, P. M.; Breeman, W. A.; Bernard, H. F.; Schaar, M.; Mooij, C. M.; Srinivasan, A.; Schmidt, M. A.; Krenning, E. P.; de Jong, M. Evaluation of a radiolabelled cyclic DTPA-RGD analogue for tumour imaging and radionuclide therapy. Int J Cancer 2000; **90**: 186-198.
22. Arap, W.; Pasqualini, R.; Ruoslahti, E. Cancer treatment by targeted drug delivery to tumor vasculature in a mouse model. Science 1998; **279**: 377-380.
23. Merrifield, R. B. Solid-phase peptide synthesis. Adv Enzymol Relat Areas Mol Biol 1969; **32**: 221-296.
24. Sastry, L.; Lin, W.; Wong, W. T.; Di Fiore, P. P.; Scoppa, C. A.; King, C. R. Quantitative analysis of Grb2-Sos1 interaction: the N-terminal SH3 domain of Grb2 mediates affinity. Oncogene 1995; **11**: 1107-1112.
25. Lung, F. D.; Li, W. C.; Chang, Y. H.; Chen, H. M. Determination of binding potency of peptidic inhibitors of Grb2-SH2 by using the protein-captured biosensor method. Protein Pept Lett 2008; **15**: 808-810.
26. Pelicci, G.; Lanfrancone, L.; Grignani, F.; McGlade, J.; Cavallo, F.; Forni, G.; Nicoletti, I.; Pawson, T.; Pelicci, P. G. A novel transforming protein (SHC) with an SH2 domain is implicated in mitogenic signal transduction. Cell 1992; **70**: 93-104.
27. Rozakis-Adcock, M.; McGlade, J.; Mbamalu, G.; Pelicci, G.; Daly, R.; Li, W.;

Batzer, A.; Thomas, S.; Brugge, J.; Pelicci, P. G.; et al. Association of the Shc and Grb2/Sem5 SH2-containing proteins is implicated in activation of the Ras pathway by tyrosine kinases. Nature 1992; **360**: 689-692.
28. Gale, N. W.; Kaplan, S.; Lowenstein, E. J.; Schlessinger, J.; Bar-Sagi, D. Grb2 mediates the EGF-dependent activation of guanine nucleotide exchange on Ras. Nature 1993; **363**: 88-92.
29. Egan, S. E.; Giddings, B. W.; Brooks, M. W.; Buday, L.; Sizeland, A. M.; Weinberg, R. A. Association of Sos Ras exchange protein with Grb2 is implicated in tyrosine kinase signal transduction and transformation. Nature 1993; **363**: 45-51.
30. Buday, L.; Downward, J. Epidermal growth factor regulates p21ras through the formation of a complex of receptor, Grb2 adapter protein, and Sos nucleotide exchange factor. Cell 1993; **73**: 611-620.
31. Schlaepfer, D. D.; Hanks, S. K.; Hunter, T.; van der Geer, P. Integrin-mediated signal transduction linked to Ras pathway by GRB2 binding to focal adhesion kinase. Nature 1994; **372**: 786-791.
32. Goudreau, N.; Cornille, F.; Duchesne, M.; Parker, F.; Tocque, B.; Garbay, C.; Roques, B. P. NMR structure of the N-terminal SH3 domain of GRB2 and its complex with a proline-rich peptide from Sos. Nat Struct Biol 1994; **1**: 898-907.
33. Pendergast, A. M.; Gishizky, M. L.; Havlik, M. H.; Witte, O. N. SH1 domain autophosphorylation of P210 BCR/ABL is required for transformation but not growth factor independence. Mol Cell Biol 1993; **13**: 1728-1736.
34. McCormick, F. Signal transduction. How receptors turn Ras on. Nature 1993; **363**: 15-16.
35. Janes, P. W.; Daly, R. J.; deFazio, A.; Sutherland, R. L. Activation of the Ras signalling pathway in human breast cancer cells overexpressing erbB-2. Oncogene 1994; **9**: 3601-3608.
36. Daly, R. J.; Binder, M. D.; Sutherland, R. L. Overexpression of the Grb2 gene in human breast cancer cell lines. Oncogene 1994; **9**: 2723-2727.
37. Oligino, L.; Lung, F. D.; Sastry, L.; Bigelow, J.; Cao, T.; Curran, M.; Burke, T. R., Jr.; Wang, S.; Krag, D.; Roller, P. P.; King, C. R. Nonphosphorylated peptide ligands for the Grb2 Src homology 2 domain. J Biol Chem 1997; **272**: 29046-29052.
38. Songyang, Z.; Shoelson, S. E.; McGlade, J.; Olivier, P.; Pawson, T.; Bustelo, X. R.; Barbacid, M.; Sabe, H.; Hanafusa, H.; Yi, T.; et al. Specific motifs recognized by the SH2 domains of Csk, 3BP2, fps/fes, GRB-2, HCP, SHC, Syk, and Vav. Mol Cell Biol 1994; **14**: 2777-2785.
39. Lung, F. D.; Long, Y. Q.; Roller, P. P.; King, C. R.; Varady, J.; Wu, X. W.; Wang, S. Functional preference of the constituent amino acid residues in a phage-library-based nonphosphorylated inhibitor of the Grb2-SH2 domain. J Pept Res 2001; **57**: 447-454.

40. Furet, P.; Gay, B.; Garcia-Echeverria, C.; Rahuel, J.; Fretz, H.; Schoepfer, J.; Caravatti, G. Discovery of 3-aminobenzyloxycarbonyl as an N-terminal group conferring high affinity to the minimal phosphopeptide sequence recognized by the Grb2-SH2 domain. J Med Chem 1997; **40**: 3551-3556.
41. Dankort, D. L.; Wang, Z.; Blackmore, V.; Moran, M. F.; Muller, W. J. Distinct tyrosine autophosphorylation sites negatively and positively modulate neu-mediated transformation. Mol Cell Biol 1997; **17**: 5410-5425.
42. Hart, C. P.; Martin, J. E.; Reed, M. A.; Keval, A. A.; Pustelnik, M. J.; Northrop, J. P.; Patel, D. V.; Grove, J. R. Potent inhibitory ligands of the GRB2 SH2 domain from recombinant peptide libraries. Cell Signal 1999; **11**: 453-464.
43. De Filippis, V.; De Antoni, F.; Frigo, M.; Polverino de Laureto, P.; Fontana, A. Enhanced protein thermostability by Ala-->Aib replacement. Biochemistry 1998; **37**: 1686-1696.
44. Myszka, D. G.; Wood, S. J.; Biere, A. L. Analysis of fibril elongation using surface plasmon resonance biosensors. Methods Enzymol 1999; **309**: 386-402.
45. Akazawa, A.; Nishikawa, K.; Suzuki, K.; Asano, R.; Kumadaki, I.; Satoh, H.; Hagiwara, K.; Shin, S. J.; Yano, T. Induction of apoptosis in a human breast cancer cell overexpressing ErbB-2 receptor by alpha-tocopheryloxybutyric acid. Jpn J Pharmacol 2002; **89**: 417-421.
46. Saceda, M.; Grunt, T. W.; Colomer, R.; Lippman, M. E.; Lupu, R.; Martin, M. B. Regulation of estrogen receptor concentration and activity by an erbB/HER ligand in breast carcinoma cell lines. Endocrinology 1996; **137**: 4322-4330.

Chapter 2

Affinity of synthetic peptide fragments of MyoD for Id1 protein and their biological effects in several cancer cells

Abstract

MyoD is a DNA binding protein capable of specific interactions specifically involved the helix-loop-helix (HLH) domain. The HLH motif of MyoD could form oligomers with the HLH motif of Id1 (the inhibitor of DNA-binding proteins) that folds into a highly stable helical conformation stabilized by the self-association. The Id family consists of four related proteins that contain a highly conserved dimerization motif known as the HLH domain. In signaling pathways, Id proteins act as dominant negative antagonists of the basic helix–loop–helix (bHLH) family of transcription factors which play important roles in cellular development, proliferation, and differentiation. The mechanism of Id proteins is to antagonize basic helix-loop-helix proteins by binding as dominant-negative HLH proteins to form high affinity heterodimers with other bHLH proteins, thereby preventing them from binding to DNA and inhibiting transcription of differentiation-associated genes. The goal of this study is to design and synthesize peptide fragments of MyoD with high affinity for Id1 in order to interrupt the interactions among Id1, MyoD and other bHLH DNA-binding proteins and to inhibit the proliferation of cancer cells. Affinity of each peptide for Id1 was determined by surface plasmon resonance (SPR) technology. The secondary structure of each peptide was studied by circular dichroism (CD) spectroscopy. Biological effects of each peptide in several cancer cells such as breast and colon cancer cells were analyzed. Results demonstrated that the peptide **3C** (H-Tyr-Ile-Glu-Gly-Leu-Gln-Ala-Leu-Leu-Arg-Asp-Gln-NH_2) not only showed high affinity for Id1, but also exhibited antiproliferative effects in HT-29 and MCF-7 cancer

cells, the IC_{50} value of **3C** was determined as 25 μM in both cells. The percentage of sub-G1 in the cell cycle of the cancer cells treated with 5 μM of **3C** was increased**,** indicating the induced apoptosis of cancer cells by **3C**. Taken together, the peptide **3C** is a promising lead compound for the development of antiproliferative agents.

Introduction

Id (the inhibitor of DNA-binding proteins or the inhibitor of differentiation) plays important role in the cell growth [1-6], differentiation [7-9], cell cycle control [10, 11], and tumorigenesis [7-9, 12]. Thus, it has been the potential target for cancer intervention [7, 9, 11, 13-16].

The Id proteins act as negative regulators of transcription factors within the basic helix–loop–helix (bHLH) family, which play an important role in cellular development, proliferation, and differentiation. bHLH proteins such as MyoD contain a DNA binding motif which contain a cluster of amino acids rich in basic residues and a dimerization motif comprised of the helix–loop–helix (HLH) domain. The Id proteins contain a HLH dimerization motif but lack a basic DNA binding motif, and Ids could associate with members of the bHLH proteins family through their HLH motif to form high-affinity heterodimers [17, 18], thereby preventing bHLH proteins from binding to DNA and inhibiting the transcription of differentiation associated genes.

The four members of the Id family (Id1-4) have similar amino acids sequences, but are subdivided with respect to expression patterns in embryo [19, 20]. Id1, the first Id protein, was named for its ability to inhibit the DNA binding of bHLH transcription factors. The associations of Id1 with E proteins and Ets proteins [21, 22] have important implications with regards to the role of Id1 in cell cycle progression [10, 11] and tumorgenesis [7-9, 12]. Id1 also plays an important role in the growth of tumor cells [1-4, 6], making it an excellent target for the design of antitumor drugs.

Ids are frequently upregulated in human cancer, their presence correlates to the proliferation, invasiveness, and neoangiogenesis [14, 23], therefore, Ids are considered as potentially versatile therapeutic targets. Recently, a peptide-conjugated Id1 antisense oligonucleotide homed to tumor endothelium was reported, which can inhibit the tumor

growth and metastasis in two different murine models [24]. However, the impact of Id inhibition in human cancer cell lines is not fully assessed.

The goal of this study is to interrupt the interactions among Id1, MyoD, and other DNA-binding proteins such as tumor suppressor-related bHLH transcription factors and to inhibit the proliferation of cancer cells. We selected MyoD as our target to design a series of peptide fragments of MyoD for the development of potent antiproliferative peptide analogs. Binding affinity of each peptide for Id1 was analyzed by surface plasmon resonance (SPR) technology developed with the BIAcore Biosensor. The secondary structure of each peptide was analyzed by circular dichroism (CD) spectroscopy. Effects of peptides in several cancer cells, including breast cancer cells (MCF-7 and MDA MB-231), colon cancer cells (HT-29 and HCT116), leukemia cells (HL-60), hepatoma cells (Hep 3B), non-small-lung cancer cells (NCI-H226), and renal cancer cells (A498), were evaluated by *in vitro* biological assays to investigate the selectivity of each peptide for the tested cancer cells.

Materials and Methods

Materials

All N_{α}-Fmoc derivatives of standard amino acids, Rink amide AM resin [4-(2',4'-Dimethoxyphenyl)-Fmoc-aminomethyl-phenoxy-acetamido-norleucylamino-methyl resin], and coupling reagents for solid phase synthesis were purchased from Anaspec Inc (San Jose, CA, US). DIEA, piperidine and TFA were purchased from Sigma (St. Louis, MO, US). DMF and acetonitrile (HPLC grade) were purchased from Tedia Company (Fairfield, OH, US). Purification of each peptide was performed by using semi-preparative scale RP-HPLC on a C_{18} column (244 × 10 mm, particle size 10 μm; Lichrospher 100 RP-18, Merck). Human Id1 was provided by Biocheck *Inc*. (Foster City, CA, U.S.A.). All of the material reagents for performing BIAcore 3000 biosensor including theSPR, CM5 sensor chip, HBS (Hepes-buffered saline; 10 mM Hepes, pH 7.4, 150 mM NaCl, 3.4 mM EDTA, 0.005% Surfactant P-20), BIAcore 3000 and the BIAevaluation software were purchased from Biacore AB, GE Healthcare company (Pollards Wood, United Kingdom). The breast cancer cells (MCF-7), colon cancer cells (HT-29 and HCT116), Leukemia cells (HL-60), hepatoma cells (Hep 3B), non-small-lung cancer cells (NCI-H226) and renal cancer cells (A498) were obtained from the American Type Culture Collection (ATCC). Culture medium, fetal bovine serum (FBS) and 1% penicillin and streptomycin were purchased from GIBCO/BRL (Grand Island, NY, U.S.A.). MTT cell proliferation kit was obtained from Boehringer Manheim (Indianapolis, IN, U.S.A.) and ELISA plate reader was performed purchased from using Versamax (Sunnyvale, CA, U.S.A.). Apoptotic cells were detected by FACS analysis, using FACS Calibur Flow Cytometer, Becton Dickinson Immunocytometry Systems (Mountain View, CA, U.S.A.)

Solid phase peptide synthesis of peptide fragments of MyoD

Each peptide fragment of MyoD was synthesized manually [25] in our laboratory by the standard solid phase peptide synthesis (SPPS) [26], using Fmoc/tBu chemistry. Briefly, the Rink amide AM resin was swelled in DMF for 10 min at room temperature, followed by the removal of the Fmoc-protecting group on the resin by treatment with 20% piperidine in DMF for 15 min, repeated twice. The N_{α}-Fmoc, side-chain-protected amino acid, Fmoc–Asn(Trt)–OH, was activated by mixing with the coupling reagent, 1-hydroxybenzotriazole/ 2-(1H-benzotriazoelyl)-tetramethyl- uronium hexafluorophosphate/N, N-diisopropylethylamine (HOBt/HBTU/DIEA, 1:1:2), for 5 min and then added to the reaction vessel for coupling with resin at room temperature for 1.5 hrs. Cycles of removing Fmoc and coupling with the subsequent amino acids were repeated to produce the desired peptide-bound resin. The crude peptide was removed from resin by TFA cleavage, lyophilized, and then purified by RP-HPLC. After purification, the peptides were characterized by MALDI-TOF-MS spectrometry and RP-HPLC.

Analysis of interactions of each peptide with the immobilized Id1 by a biosensor

We have reported applications of surface plasmon resonance (SPR) technology in analyzing the interactions of Grb2 SH2 protein with its peptidic antagonists and in determining the dissociation equilibrium constant (K_D) of each synthetic peptide [25, 27, 28]. In this study, Id1 was immobilized on the surface of biosensor chip and then the binding interaction of Id1 with each synthetic peptide was analyzed to determine the binding affinity of each peptide for Id1.

The surface of CM5 chip was activated by the addition of 0.1 M NHS/0.4 M EDC (v/v = 1, 35 μL) at the flow rate of 5 μL/min. Id1 (30 μg/mL, 200 μL) was injected for immobilization on the surface of sensor chip. Finally, 35 μL of ethanolamine

hydrochloride (0.1 M, pH 8.5) was injected for blocking the activated surface. In this study, purified peptides were diluted into various concentrations with HBS buffer, and each sample was introduced separately onto the Id1-immobilized CM5 chip at the flow rate of 30 μL/min for 3 min. The binding interaction between each peptide and the Id1 was detected and displayed as a sensorgram by plotting the resonance unit (RU) against time, at least, in triplicate. Detected changes of RU represent the association and dissociation of Id1, and the data was analyzed using BIA evaluation software (Biacore AB, Pharmacia, Uppsala, Sweden) to determine the equilibrium constants of each peptide. The dissociation equilibrium constants (K_D) were calculated as the ratio of dissociation (k_d) and association (k_a) rate constants. The K_D of the binding system could also be determined using the Scatchard analysis by plotting RU/[peptide concentration] vs. RU to yield a linear line with the slope equal to $-1/K_D$. RU is the maximal resonance unit at a given peptide concentration.

Analysis of the secondary structure of each peptide by CD spectroscopy

Solutions of four peptide analogs (3A, 3B, 3C, and 3D) were prepared at the same concentration (3.7 μM, in 0.1M phosphate buffer, pH 7.2). The secondary structures of these peptides were analyzed by circular dichroism (CD) spectroscopy using Jasco-715 (Jasco Inc., Easton, MD, USA). The CD spectrum of each peptide solution was recorded at room temperature, and for each CD spectrum, 2 scans were accumulated using a step resolution of 1 nm, a bandwidth of 1 nm, a response time of 2 sec, a scan speed of 100 nm/min, and a sensitivity of high. The CD spectrum of the buffer was subtracted from that of each peptide in order to eliminate interferences from the cell, the solvent, or the optical equipment.

Determination of the cell viability by using the cell proliferation assay

The breast cancer cells (MCF-7 and MDA MB-231), colon cancer cells (HT-29 and

HCT116), leukemia cells (HL-60), hepatoma cells (Hep 3B), non-small-lung cancer cells (NCI-H226) and renal cancer cells (A498) were obtained from the American Type Culture Collection (ATCC). MCF-7 cells were maintained in Dulbecco's modified Eagle's Medium (DMEM) (GIBCO/BRL, NY, U.S.A.) with 10% fetal bovine serum (FBS; GIBCO/BRL), 1% penicillin and streptomycin (GIBCO/BRL) at 37°C, 5% CO_2, HT-29, HCT116, HL-60, Hep 3B, NCI-H226 and A498 cell lines were cultured in RPMI-1640 (GIBCO/BRL, NY, U.S.A.) with 5% fetal bovine serum (FBS; GIBCO/BRL), 1% penicillin (100 units/ml) (GIBCO/BRL) and 1% streptomycin (GIBCO/BRL) 37°C, 5% CO_2.

The inhibitory effect of each peptide on the proliferation of various cancer cells was determined using the MTT assay. Briefly, HCT116, HT 29, Hep 3B, NCI-H226, A498, MDA MB-231 and MCF-7 cells (10^4/well) were loaded into 96-well culture plates. After 24 hrs, cells were treated with fresh medium containing various concentrations of each peptide for 24 hrs and 48 hrs. The suspension cells, HL 60 (10^5/well), were seeding into 24-well plates and treated with each peptide for 48 hrs. The peptide-treated and the control (cancer cells without treatment with any peptides) were washed once with PBS and reacted with the MTT solution (Boehringer Manheim, Indianapolis, IN) at 37°C for 2 hrs to produce the formazan salt. Finally, the formazan salt formed in each cultured cells was dissolved in DMSO, and the optical density (OD) value of each solution was measured at 570 nm using an ELISA reader (Versamax, Sunnyvale, CA, U.S.A.).

The OD value detected for the control was plotted on the x-axis, and considered as 100% of viable cancer cells. The OD value detected for the solution from the peptide-treated cells was also plotted on the x-axis, designated as proliferation (%control), to demonstrate the effect of each peptide on the viability of the related cancer cells.

The IC_{50} value represents the concentration of a compound/molecule that caused 50% inhibition of certain reaction, such as some biological processes or proliferation of cells. In the MTT assay, we recorded the concentrations of peptides and the proliferation of cancer cells (%control) as the x-values and the y-values, respectively. Based on these known x-values and y-values, the IC_{50} value of each peptide can be calculated by using linear regression. The equation is $a+bx$, where: $a = \bar{y}-b\bar{x}$, *and* $b = \frac{\Sigma(x-\bar{x})(y-\bar{y})}{\Sigma(x-\bar{x})^2}$ and where $\bar{x}$ and $\bar{y}$ are the means of the AVERAGE of our known x-values and y-values, respectively. This formula can be used in Excel's built-in forecasting to calculate the IC_{50} value of our peptide by setting 50% as the y-value.

Flow cytometric analysis of the DNA content and the cell cycle in cancer cells

Apoptotic cells were detected by FACS analysis of nuclear propidium iodide stained cells. The cells (1 x 10^6 cells) were grown in 5 mL of DMEM containing 10% FBS for 24 hrs and 48 hrs in the presence of 5 μM of the peptide **3A**. For flow cytometry analysis, cells were trypsinized and pelleted by centrifugation. After removal of the supernant, the pelleted cells was fixed by slowly addition of 5 mL of the PBS solution containing 70% ethanol (it took about 30 min for completion) at -20°C. The cells in the suspension were then centrifuged to remove the ethanol, and the pellets of cells were washed with PBS twice. The cells were permeabilized and stained by adding 500 μL of propidium iodide solution (50 μg/mL propidium iodide / 1% Triton X-100 / 0.1 mg/mL RNase in PBS) into the cells, and then the treated cells were incubated for 40 min at 37 ^oC. The stained cells were subjected to cell cycle analysis by using the Modifit cell cycle analysis software developed with a FACSCalibur Flow Cytometer (Becton Dickinson Immunocytometry Systems, Mountain View, CA, U.S.A.).

Statistical Analysis

All values shown are means ± SEM (standard error of the mean). Differences between

treated groups and controls were analyzed by one-way ANOVA followed by Dunnett's multiple comparison tests. Differences in cell growth were analyzed by Student's *t*-test. Significance was accepted at $p < 0.05$.

Results

Design and synthesis of peptide fragments of MyoD

Previous studies using electrophoretic mobility shifts assay (EMSA), circular dichroism (CD) spectroscopy, and sedimentary equilibrium (SE) ultracentrifigation helped determine the DNA-binding and oligomerization equilibria of Id, MyoD and E47 motifs [29]. It was found that homodimers of bHLH proteins such as MyoD are known to activate tissue-specific genes. MyoD is a DNA binding protein capable of specific interactions specifically involved in the helix-loop-helix (HLH) domain. The HLH domain of Id has stronger cooperativity and affinity for heterotetramerization with the bHLH of MyoD [29, 30], resulting in inhibition of its DNA-binding activity. Our goal is to inhibit the proliferation of cancer cells by interrupting the interactions of Id1 with DNA-binding proteins such as MyoD and E2A and by affecting the transcription and gene expression through the actions of our designed peptides (Figure 2-1).

Mutagenesis experiments performed with MyoD protein have demonstrated that the bHLH domain of MyoD is required for dimerization and the basic region of MyoD mediates the DNA-binding. Because our goal is to inhibit the proliferation of cancer cells through the interruption of binding interactions among MyoD, Id1, and other bHLH proteins, we designed and synthesized three peptide fragments of MyoD (peptides 1A, 2A, and 3A) corresponding to the basic region, helix1 motif, and helix2 motif of MyoD, respectively (Figure 2-2).

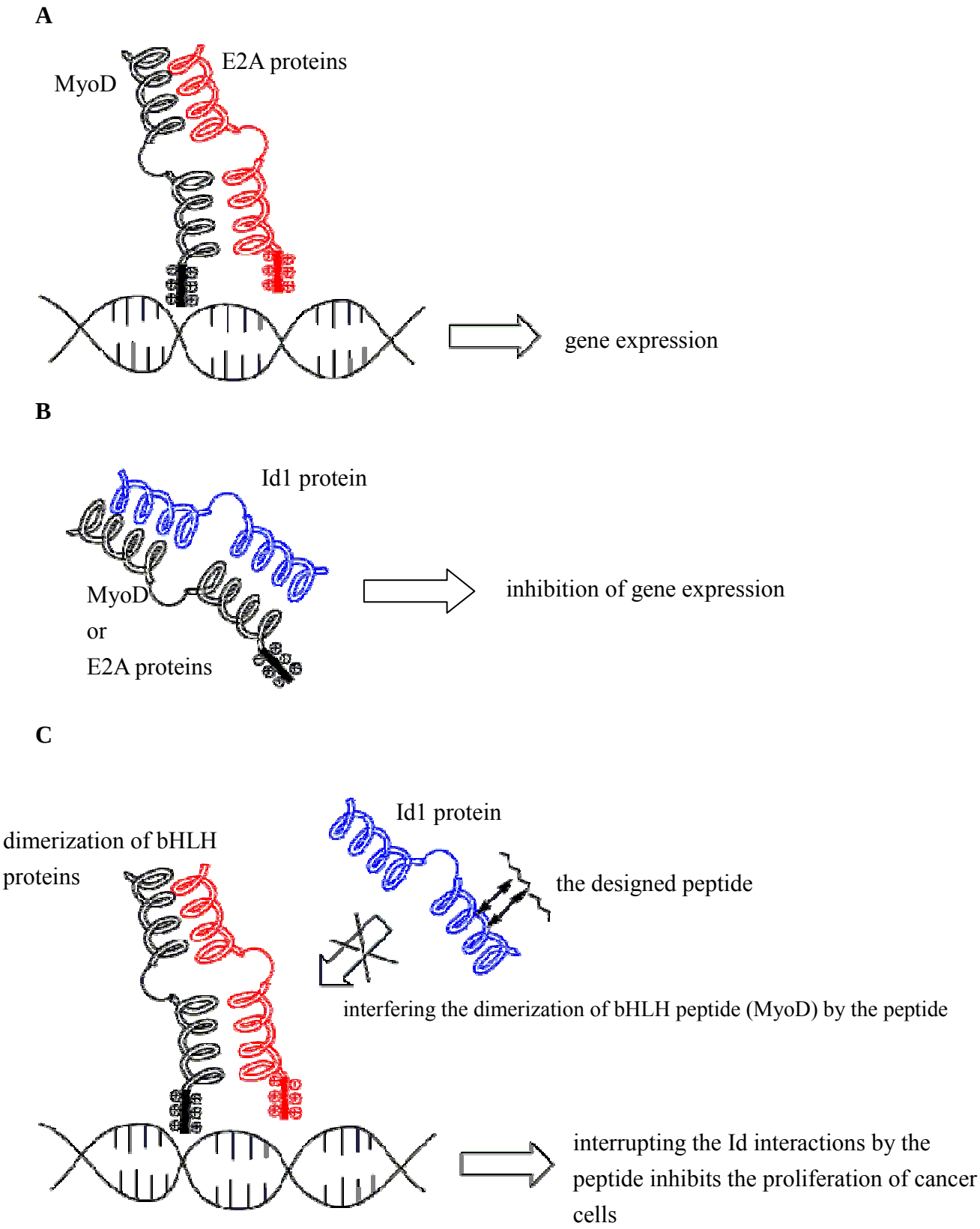

Figure 2-1. Proposed mechanism of the inhibitory effect of a designed peptide on MyoD-Id1 interactions. (A) A heterodimer of the E2A proteins and MyoD mediates the DNA binding. (B) The inhibitor of DNA binding protein (Id1) forms the Id1/E2A or

Id1/MyoD heterodimer to control the gene expression. Id exerts its dominant negative effect on sequestering the ubiquitously expressed MyoD. (C) Our proposed mechanism for interrupting the Id1 functions by the designed peptide. We propose that the association/interaction of the designed peptide with Id1 should interrupt the binding of Id to bHLH family, leading to the inhibitory effect on the proliferation of cancer cells.

The affinity (or binding potency) of each peptide for Id1 was determined by analyzing the sensorgrams obtained by interacting of each peptide with the immobilized Id1 using the surface plasmon resonance (SPR) technology developed with the biosensor-BIAcore 3000. Results indicated that among the peptides with the same concentration (50 μM), the peptide **3A,** which is the helix2 region within the C-terminal amino acid sequence of MyoD, exhibited the highest binding potency to Id1 (Figure 2-3). Therefore, we selected the peptide **3A** as our lead compound and designed a series of N-terminal truncated peptide analogs of **3A** (Figure 2-4) in order to develop smaller and more potent peptides with enhanced binding affinity for Id1 and/or increased antiproliferative effects in cancer cells. Synthesized peptides were purified by RP-HPLC and characterized by MALDI-TOF-MS spectroscopy (Table 2-1),

(A)

MyoD

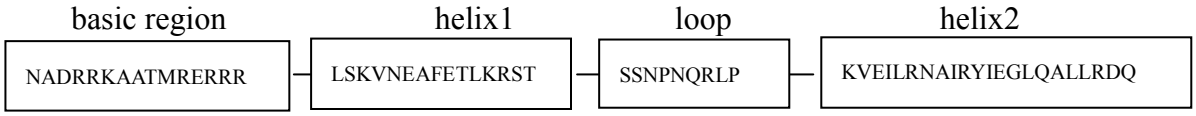

(B)

H-Asn-Ala-Asp-Arg-Arg-Lys-Ala-Ala-Thr-Met-Arg-Glu-Arg-Arg-Arg-NH_2 (**1A**)

H-Leu-Ser-Lys-Val-Asn-Glu-Ala-Phe-Glu-Thr-Leu-Lys-Arg-Ser-Thr-NH_2 (**2A**)

H-Lys-Val-Glu-Ile-Leu-Gln-His-Val-Ile-Asp-Tyr-Ile-Glu-Gly-Leu-Gln-Ala-Leu-Leu-Arg-Asp-Gln-NH_2 (**3A**)

Figure 2-2. Designed peptide fragments of the bHLH (basic-helix-loop-helix) domain of MyoD. (A) Amino acid sequences of bHLH domain of MyoD; (B) amino acid sequences of peptides **1A**, **2A**, and **3A**.

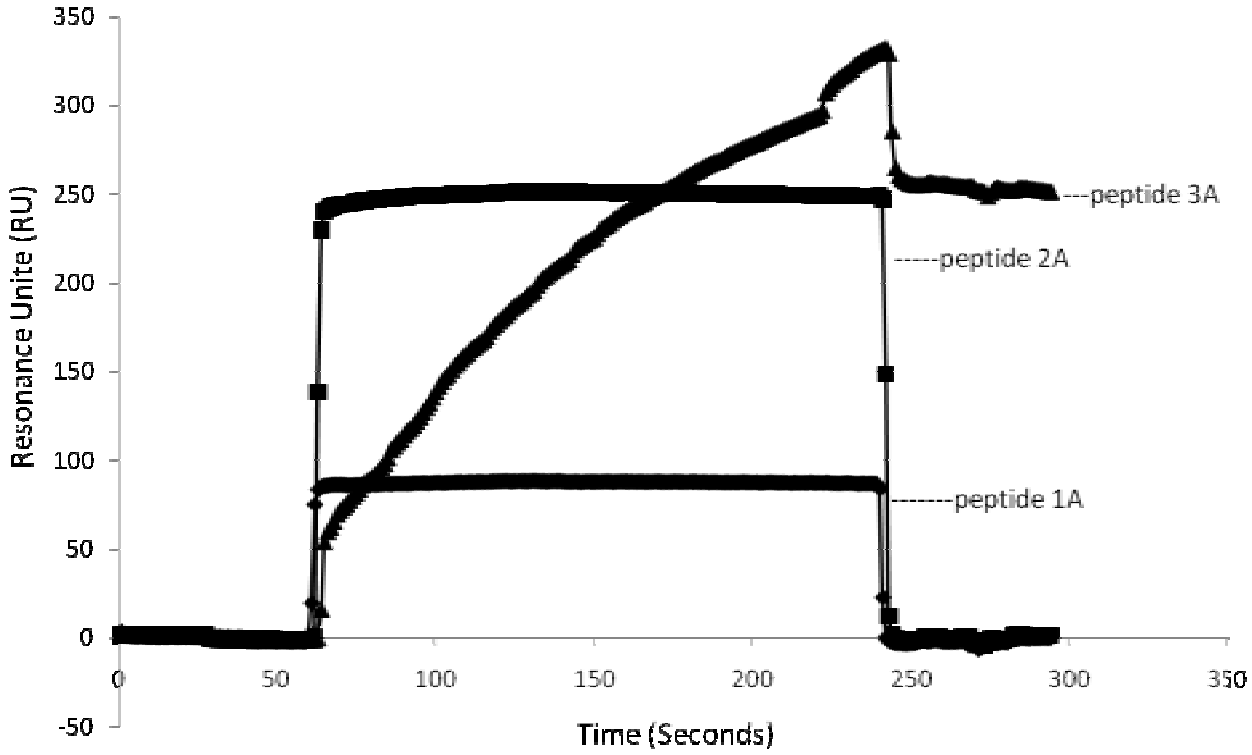

Figure 2-3. An overlay plot of the binding curves showing the interactions of peptides 1A, 2A and 3A with the immobilized Id1. Peptide solutions (50 μM in 10 mM HEPES, 0.5 mM MnCl2, 0.5 M CaCl2 and 0.05% surfactant, pH 7.4) were injected. The bound peptide was dissociated by 30 mM NaCl (20 μL/min).

H-Lys-Val-Glu-Ile-Leu-Gln-His-Val-Ile-Asp-Tyr-Ile-Glu-Gly-Leu-Gln-Ala-Leu-Leu-Arg-Asp-Gln-NH_2 **(3A)**

H-Leu-Gln-His-Val-Ile-Asp-Tyr-Ile-Glu-Gly-Leu-Gln-Ala-Leu-Leu-Arg-Asp-Gln-Cys-NH_2 **(3B)**

H-Tyr-Ile-Glu-Gly-Leu-Gln-Ala-Leu-Leu-Arg-Asp-Gln-Cys-NH_2 **(3C)**

H-Ala-Leu-Leu-Arg-Asp-Gln-NH_2 **(3D)**

Figure 2-4. Amino acid sequences of designed peptides **3A**, **3B**, **3C**, and **3D**.

In order to synthesize cyclic potent peptide for future structure-activity relationships study, the peptides **3B** and **3C** was designed with an additional Cys at the C-terminal of each peptide.

Table 2-1. Physicochemical characterization of the designed peptides

Peptide	RP-HPLC (Rt, min)	Purity (%)	Theoretical Mass (Daltons)	MALDI-TOF-MS (Daltons)
3A	16.35	95	2610.9	2610.9
3B	17.19	96	2244.5	2243.4
3C	17.95	94	1520.7	1521.2
3D	15.5	95	713.7	714.5

Analysis of interactions between each peptide and the immobilized Id1 by a biosensor

The interaction between each peptide and the immobilized Id1 was analyzed using SPR technology. The Id1 protein was immobilized on the sensor chip for monitoring the interaction between each designed peptide and Id1 in real time (Figure 2-5).

The affinity of each peptide for Id1 was determined as the SPR-derived K_D value (Table 2-2) that indicates the affinity (or binding potency) of each peptide for Id1. Among the four peptides, **3A**, **3B**, **3C**, and **3D**, the peptide **3C** with the lowest K_D value (12.5 μM) exhibited the highest affinity for Id1, while the peptide **3D (**K_D = 367.2 μM) exhibited the lowest affinity for Id1.

Analysis of the secondary structure of each peptide by CD spectroscopy

Circular dichroism (CD) spectroscopy was applied to analyze the secondary structure of synthetic peptides **3A**, **3B**, **3C,** and **3D**. A maximum signal at 190 nm and two minima signals at 203 nm and 221 were characteristics of the peptides **3A**, **3B**, and **3C**. Such a CD-spectra pattern has been generally attributed to a partially helical conformation. The contents of α-helix and β-strand presented in these peptides were estimated by using the K2D2 method [31]. Results indicate that the presence of 8.42%, 15.43%, and 8.41% helix were characterized in peptides **3A**, **3B,** and peptide **3C,** respectively (Figure 2-6).

Antiproliferative effects of peptides in various cancer cells

The SPR-derived dissociation constant (K_D) of each peptide indicates the potency of each peptide for binding to the Id1 protein, however, it may not reflect the biological effects of peptides in the intact cells, because peptides must cross the cell membranes in order to interact with their target proteins. Thus, it is necessary to perform the cell viability assay with peptides to investigate their antiproliferative effects in cancer cells.

The dysregulated expression of Id in various human primary tumor biopsies originating from the digestive system, neural tissue, or the reproductive system has been analyzed [13], and the colorectal carcinoma was found to be overexpressed with Id1 [32], thus, the colon cancer cell (HT-29) was the first cancer cell we chosed to evaluate the antiprolifeartive effect of our synthetic peptides.

Colon cancer cells (HT-29) were treated with 100 μM of peptides **3A**, **3B**, **3C**, and **3D** separately for 24 hrs, and then analyzed by MTT cell viability assay. The formazan product of MTT assay was analyzed for quantification of the viability of cells. Peptide **3A**, **3B** and **3C** were found to exhibit significantly inhibitory effect in HT-29 cells (Figure 2-7A), while peptide **3D** enhanced the proliferation of HT-29 cells (the cell viability was increased by additional 60% higher than the control). The peptide **3C** that exhibited the most significant anti-proliferative effects in HT-29 cells was served as our lead compound for further biological studies.

In order to determine the IC_{50} value of peptide **3C,** the HT-29 cells were treated with various concentrations of peptide **3C** (5, 20, 40, 60 and 80 μM) for 24 hrs and 48 hrs, and then the peptide-treated cells were assayed by MTT assay for the cell viability, proliferation (% of control), as shown in Figure 2-7B. The IC_{50} of peptide **3C** for 24 hr- and 48 hr-treated cells were calculated as 27 μM and 25 μM, respectively.

To study the biological effect of peptide **3C** in breast cancer cells, MCF-7 breast cancer cells were also treated with various concentrations of peptide **3C** (5, 20, 40, 60 and 80 μM) for 24 hrs and 48 hrs, and then assayed for their viability. The IC_{50} for 24 hr- and 48 hr-treated MCF-7 cells were calculated as 30 μM and 25 μM, respectively (Figure 2-7C).

A

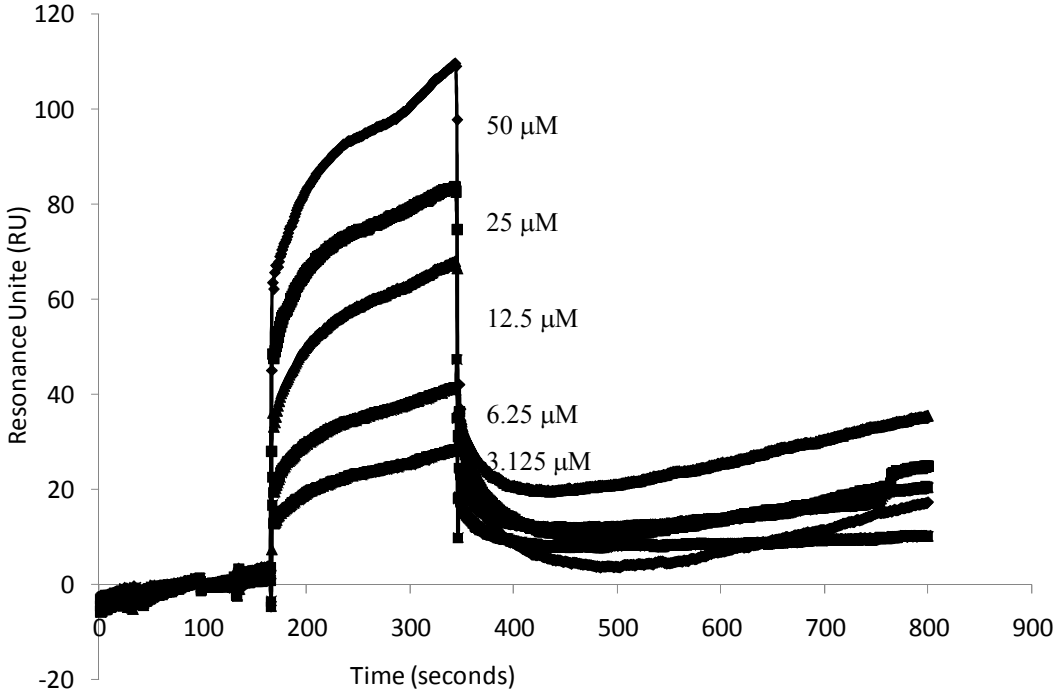

B

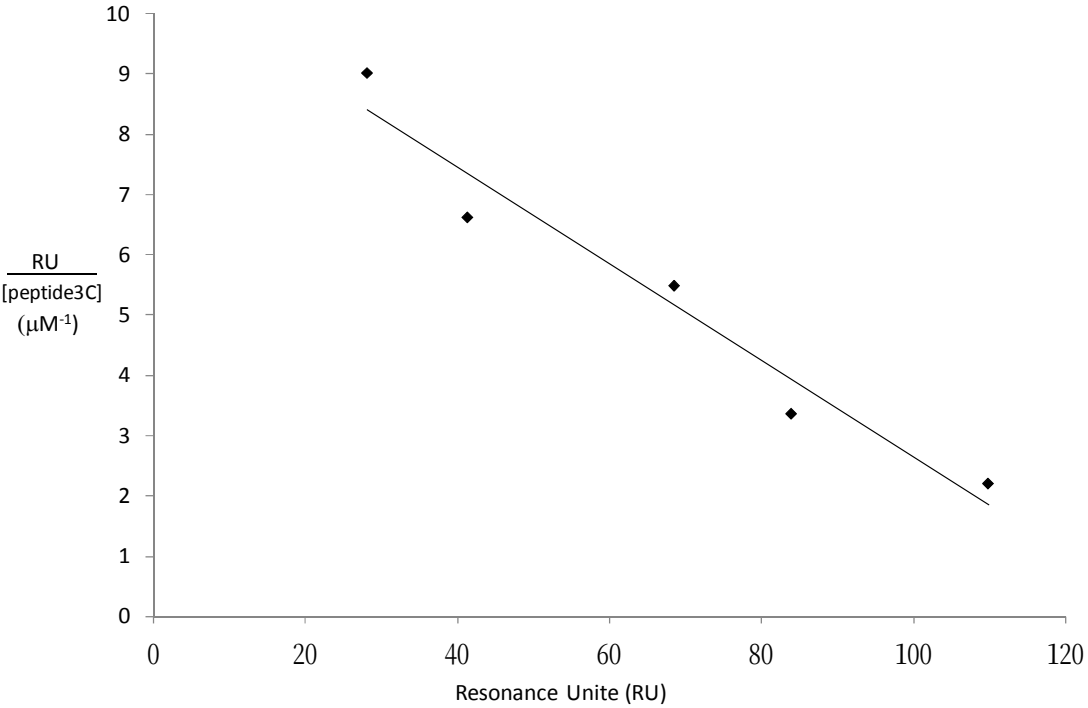

Figure 2-5. Analysis of binding affinity of the peptide 3C for the immobilized Id1 using surface plasmon resonance technology. (A) Representative sensorgrams of binding of different concentrations of peptide 3C (50, 25, 12.5, 6.25 and 3.125 μM) to the

immobilized human Id1 which derived from a 1:1 binding model. From the global fits k_{on} = 959 $M^{-1}S^{-1}$, k_{off} = 0.0179 S^{-1}, and the K_D value was determined as 18.6 μM by using BIA-software. The X- and Y-axis of sensorgram are time (seconds) and resonance unit (RU); (B) Scatchard plot of the binding data determined the K_D value as 12.5 μM by plotting the RU/ [peptide concentration] versus RU, and then calculating the slope which is equal to $-1/K_D$. The X- and Y-axis of plot are RU and RU/ [peptide concentration].

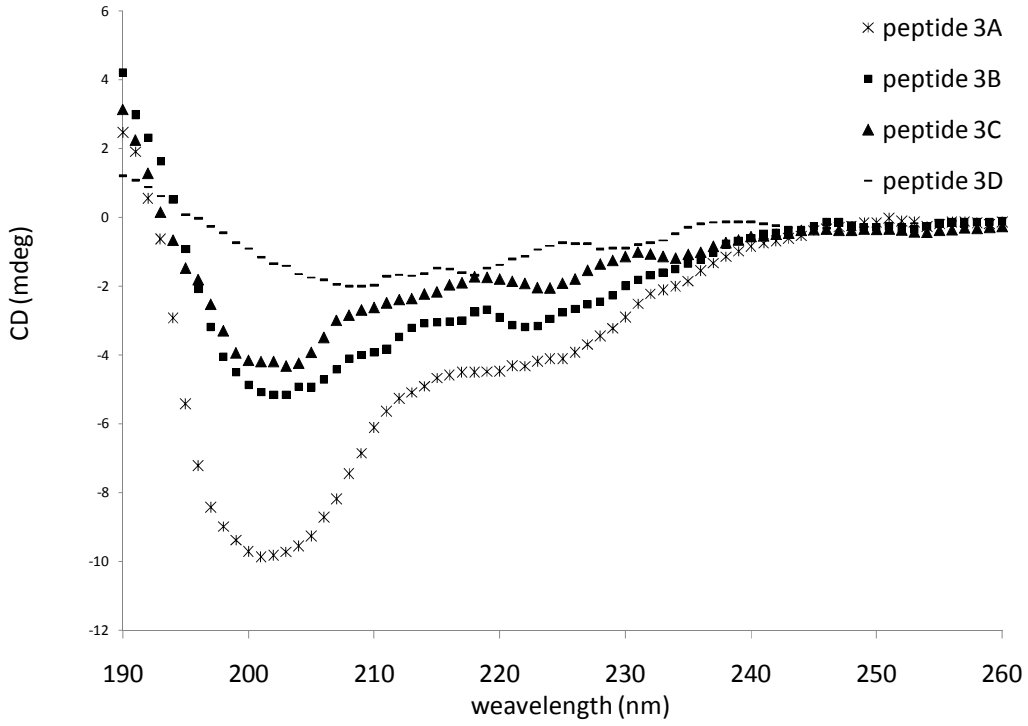

Figure 2-6. The spectra of the synthesized peptides (**3A**, **3B**, **3C** and **3D**) detected by circular dichroism (CD) spectroscopy.

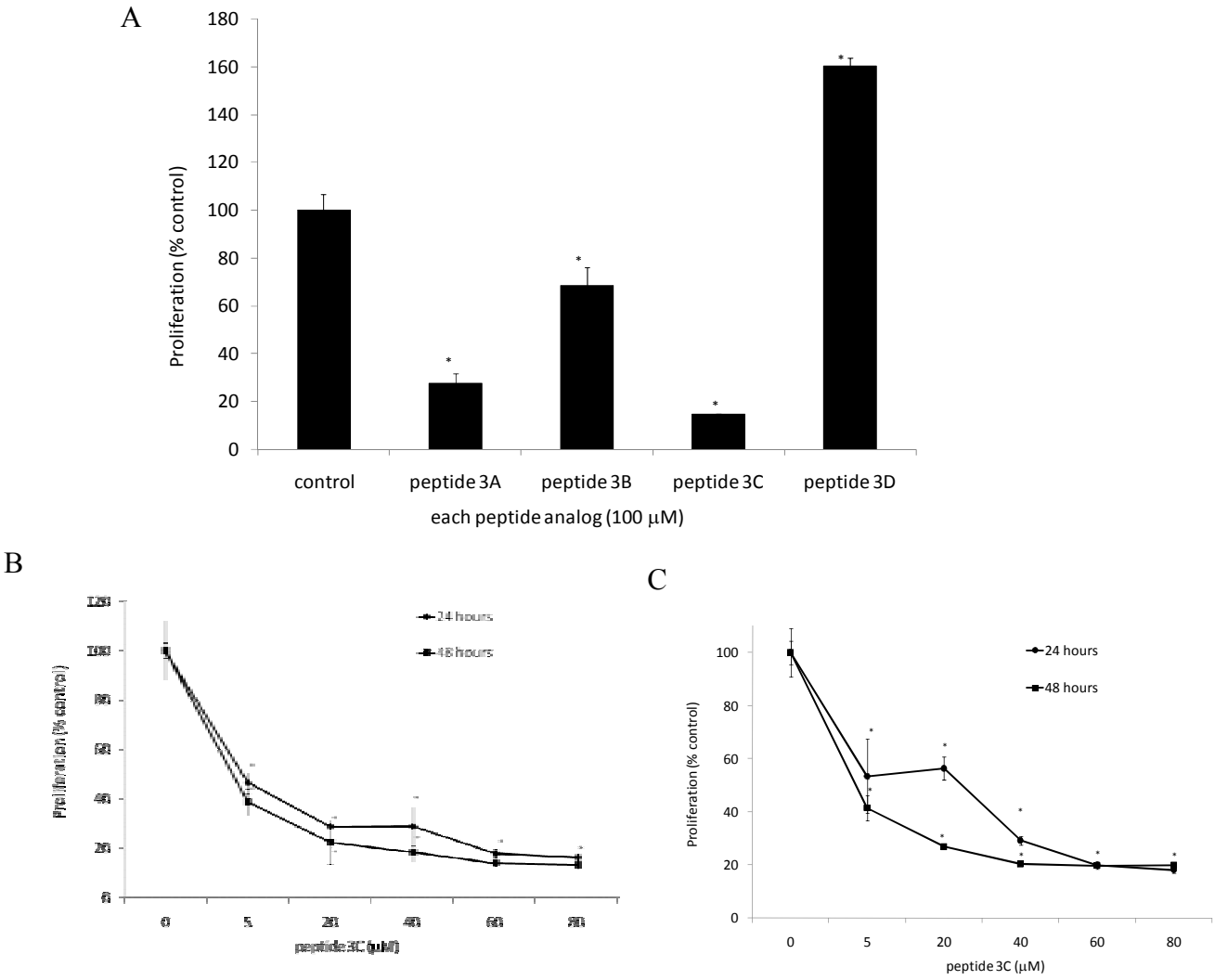

Figure Figure 2-7. The cell viability of peptide-treated human colon cancer cells and breast cancer cells. (A) Human colon cancer cells HT-29 were treated with 100 μM of peptide **3A**, **3B, 3C,** and **3D** for 24 hrs; (B) Human colon cancer cells HT-29 were treated with 5, 20, 40, 60, and 80 μM of **3C** for 24 hrs and 48 hrs; (C) Human breast cancer cells MCF-7 were treated with 5, 20, 40, 60, and 80 μM of **3C** for 24 hrs and 48 hrs. The Cell viability of peptide-treated cancer cells was determined by the MTT assay. Data are the mean value ± SD (the standard deviation) of three independent experiments. *$p < 0.05$ compared with control.

Table 2-2. Equilibrium dissociation constants of the designed peptides

Peptide	K_D[a] (μM)
3A	30.6 ±7.5
3B	38.4 ± 2.3
3C	12.5 ± 4.6
3D	367.2 ± 19.2

[a]K_D : equilibrium dissociation constant

To investigate the selectivity of peptides for various cancer cells, several cancer cells including leukemia (HL-60), colon cancer (HCT116), hepatoma (Hep 3B), non-small-lung cancer (NCI-H226) and renal cancer (A498) cells were treated separately with peptides **3A** and **3C** for 48 hrs, and then assayed for the cell viability by MTT assay. As summarized in Table 2-3, the peptide **3A** exhibited antiproliferative effects in leukemia (HL-60) and colon cancer (HCT116) cells (IC_{50} = 30 μM and 23.9 μM, respectively), and the peptide **3C** also exhibited antiproliferative effects in Leukemia (HL-60) and colon cancer (HCT116) cells (IC_{50} = 30 μM and 30 μM, respectively). The IC_{50} value of peptides 3**A** and **3C** were higher than 30 μM for hepatoma (Hep 3B), non-small-lung cancer (NCI-H226) and renal cancer (A498) cells. These results suggest that peptides 3**A** and **3C** can selectively inhibit the leukemia and colon cancer cells.

The Id1 was demonstrated as a selective mediator of lung metastatic colonization in the triple negative (TN), i.e., lacking expression of estrogen receptor and progesterone receptor, and lacking Her2 (human epidermal growth factor receptor 2) amplification, subgroup of human breast cancer. Therefore, we attempt to investigate the inhibitory effect of our most potent peptide **3C** in the invasive cells. MDA-MB-231 breast cancer cells (the TN cells) were treated with various concentrations of peptide **3C** (5, 10, 20, 40, 60 and 80 μM) for 24 hrs and 48 hrs, and the IC_{50} for 24 hr- and 48 hr-treated cells were determined as 73 μM and 60 μM, respectively (Figure 2-8).

In conclusion, our synthetic peptides exhibited antiproliferative effects not only in HT-29 colon cancer cells and MCF-7 breast cancer cells, but also in HL-60 leukemia cells and HCT116 colon cancer cells.

For the development of promising anticancer agents, it is important not only to screen the selectivity (or specificity) of **3C** among several cancer cells, but also to assay if **3C**

exhibited any cytotoxicity in non-cancer cells because Id is not overexpressed in non-cancer cells. Thus, the effect of peptide **3C** on non-cancer cells (human skin cells, HS-68) was tested, and results indicated that the peptides **3C** did not exhibited significant inhibitory effects on the proliferation of HS-68 at the concentrations of 25, 50, 75 and 100 μM (Figure 2-9).

Table 2-3. The inhibitory effects of peptides on the proliferation of human cancer cells

Peptide	**IC_{50} (μM)**				
	HL-60[a]	**HCT116[b]**	**Hep 3B[c]**	**H226[d]**	**A498[e]**
3A	30 μM ±4.1	23.9 μM ±4.6	81.3 ±2.6	64.2 ±3.7	82.7 ±2.6
3C	30 μM ±5.5	30 μM ±2.8	103.4 ±1.7	(104.9 ±3.6)	91.3 ±0.9

[a]HL-60, Leukemia cells; [b]HCT116, colon cancer cells; [c]Hep 3B, hepatoma canaer cells; [d]NCI-H226, non-small-lung cancer, and [e]A498, renal cancer cells. All of the cancer cells were treated with the peptides **3A** and **3C** seperatively for 48 hrs, then their inhibitory effects on the proliferation of the peptide-treated cells were analyzed using the MTT assay. Data are the mean value ± SD of three independent experiments. *$p < 0.01$ compared with control.

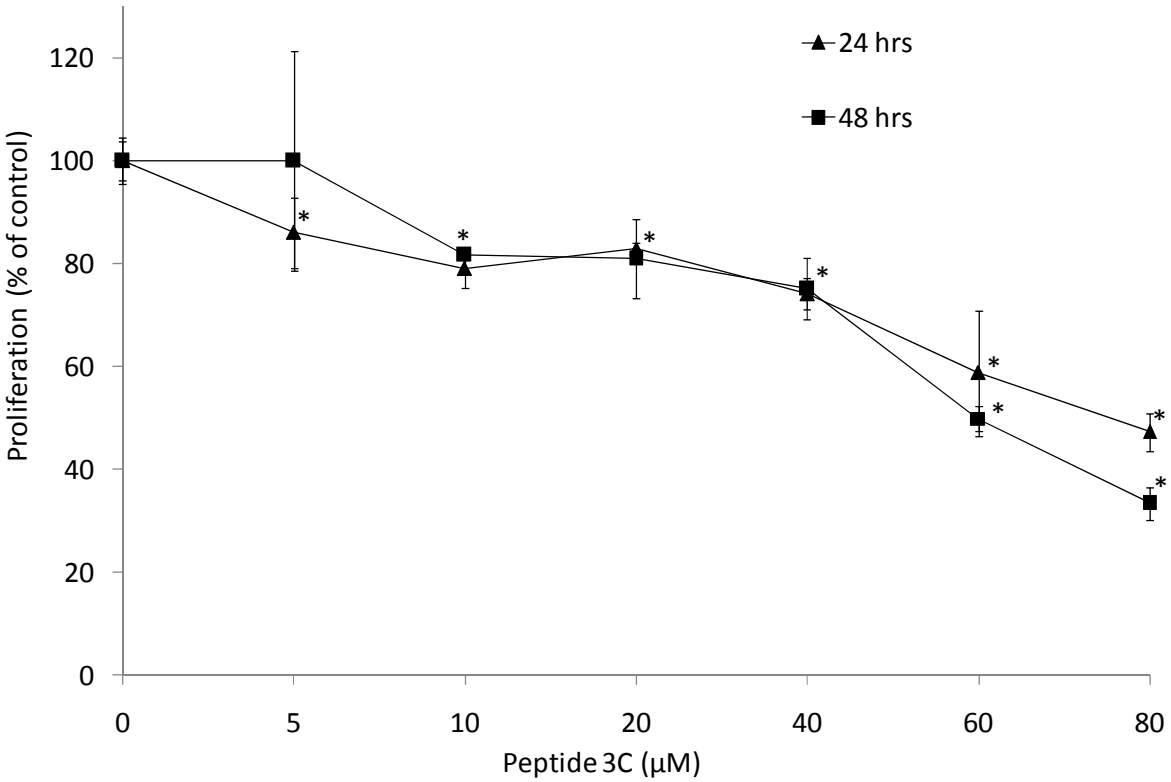

Figure 2-8. The cell viability of peptide-treated human breast cancer cells. Human breast cancer cells MDA-MB-231 were treated with 5, 10, 20, 40, 60, and 80 μM of peptide **3C** for 24 hrs and 48 hrs. The cell viability of was determined by the MTT assay. Data are the mean value ± SD of three independent experiments. *$p < 0.05$ compared with control.

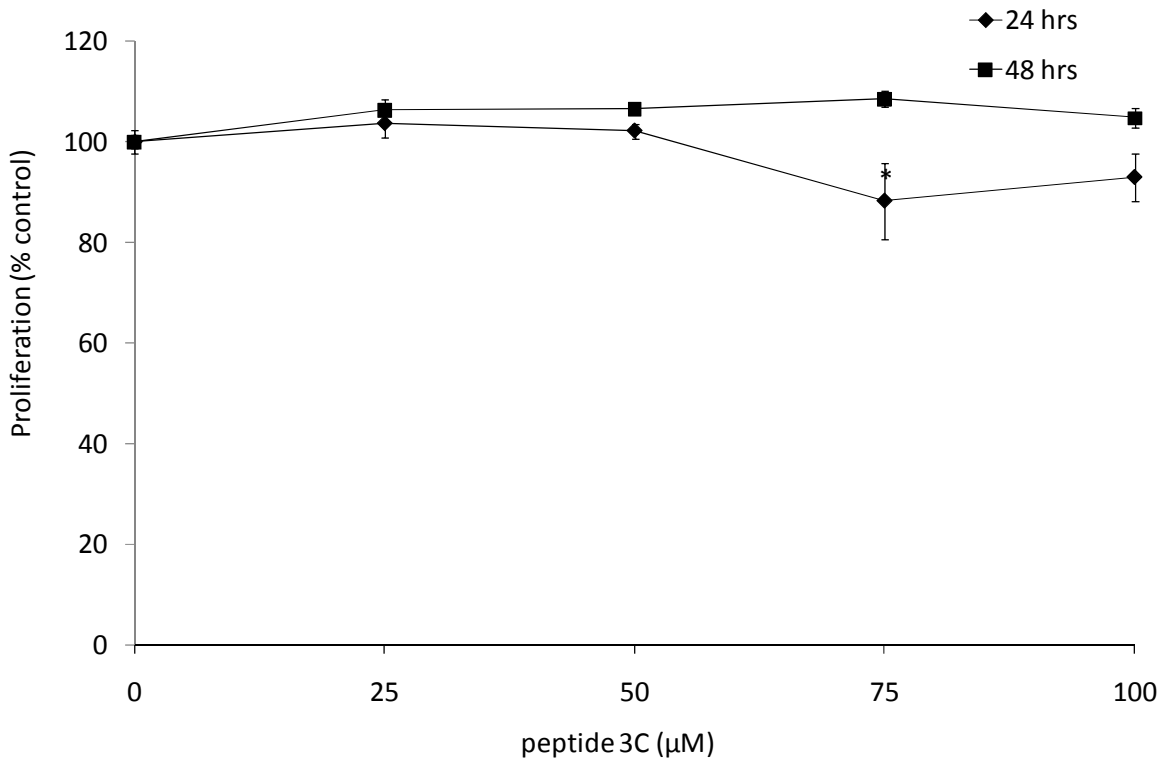

Figure 2-9. The cell viability of peptide-treated human skin cancer cells. Human skin cells HS-68 were treated with 0, 25, 50, 75 and 100 μM of the peptide **3C** for 24 hrs and 48 hrs. The cell viability of peptide-treated cells was determined by the MTT assay. Data are the mean value ± SD of three independent experiments.

Effects of the peptide 3C on the DNA content and the progression of cell cycle

Signals from single cells (size, granularity or fluorescence) can be measured by flow cytometry as they flow in a fluid stream one by one through a laser point. Flow cytometry data are easy to visualize and to compare between samples. In this study, by staining the cells with nuclear propidium iodide stain, the apoptotic cells can be detected.

Cancer cells treated with peptide **3C** (5 μM) for 24 hrs and 48 hrs were harvested, and their DNA contents were analyzed by flow cytometry. After 48-hour treatment of MCF-7 cells with the peptide **3C,** a pronounced loss of G1 phase cells was found, and the proportion of G1 phase cells decreased from 65.61 to 45.70% (Figure 2-10A, up).

The proportion of cells in sub-G1 phase increased from 11.82% to 22.13% and from 1.61 to 10.39% for 24 hr- and 48 hr-peptide treated cells, respectively (Figure 2-10A). The percentage of cells in G2/M phase increased markedly from 23.34% to 36.43% after the 48-hr incubation. These results are in agreement with the MTT results, indicating the antiproliferative effect of the peptide **3C** on breast cancer cells was correlated with its induction of the apoptosis of cancer cells. It also demonstrated that the peptide **3C** would arrest at the G2/M phase of the cell cycle in MCF-7 cells.

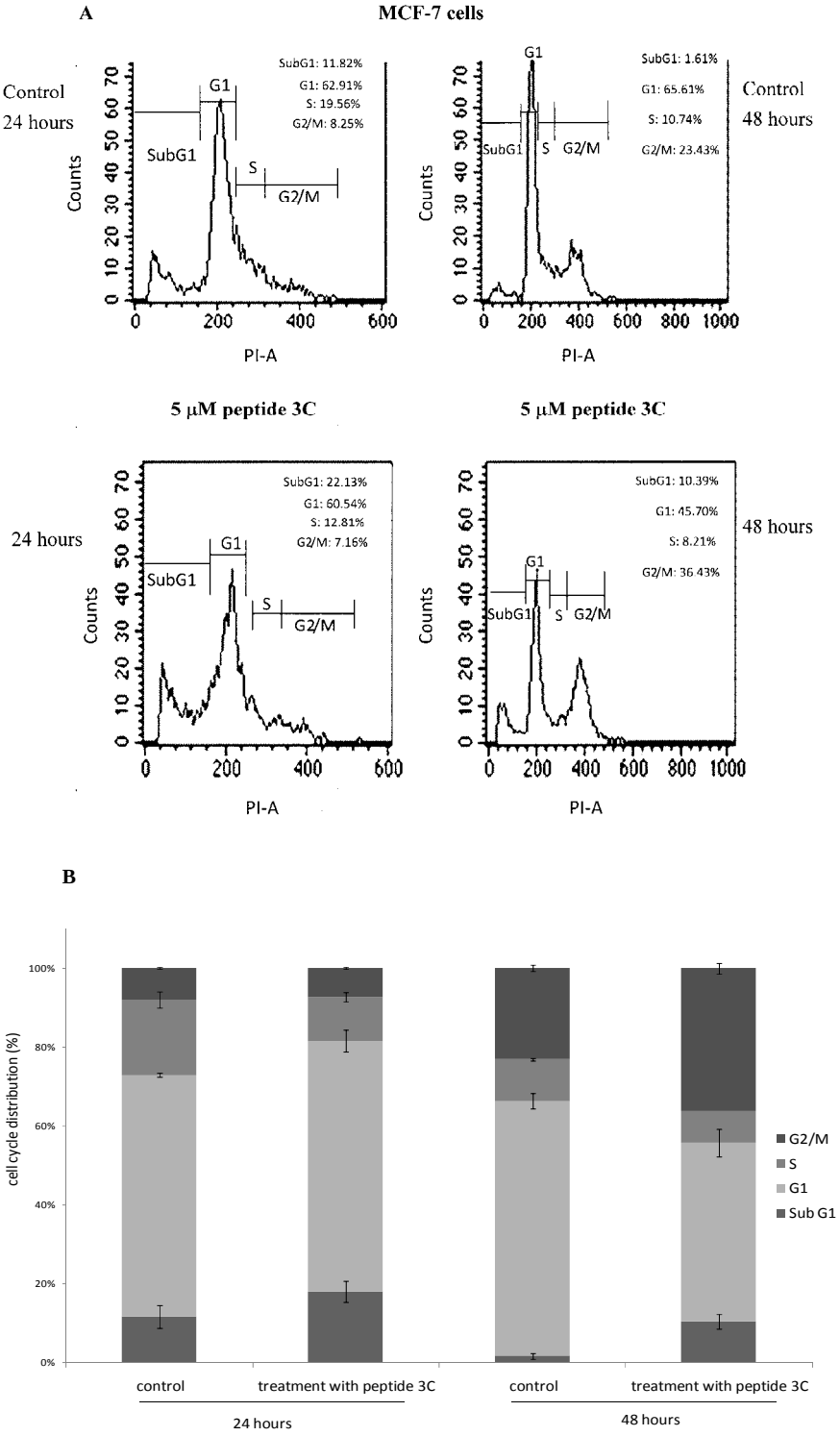

Figure 2-10. Effects of peptide **3C** on the cell cycle of breast cancer cells (MCF-7). The cells were incubated with 5 μM of peptide **3C** for 24 hrs and 48 hrs, and then analyzed by flow cytometry. (A) The FACS profiles of MCF-7 cancer cells and cancer cells treated with **3C**; (B) Effect of **3C** on the distribution of MCF-7 cells in distinct phases in the cell cycle. MCF-7 cells were continuously exposed to **3C** at the indicated concentrations for 24 hrs or 48 hrs. The graph represents the mean value ± SD of two independent experiments.

Design and analysis interactions of Id1 of peptide 3C substrate by alanine-scanning strategies

Based on the results of SPR and cell proliferation assays, and in order to find preference residues of peptide **3C** for Id1. We designed the substrate peptide analogs which similar to the sequence around interactions between peptide **3C** and Id1 (Table 2-4). SPPS method produced the N-terminal replaced peptide **3C** analogs by alanine-scanning strategies. The binding interaction of Id1 with each alanine-replaced synthetic peptide was analyzed with SPR-based method.

In this study, purified peptides were diluted into various concentrations with HBS buffer, and each sample was introduced separately onto the Id1-immobilized CM5 chip at the flow rate of 30 μL/min for 3 min. The binding interaction between each peptide and the Id1 was detected and displayed as a sensorgram by plotting the resonance unit (RU) against time, at least, in triplicate. Detected maxima changes of RU represent the association of peptides and Id1, and the data was plotted by delta RU against concentrations of each peptide (Figure 2-11). The plot yields a linear line with the slope which relate to binding affinity of given peptide to Id1.

Among all the synthetic peptides, peptide 3CA2 exhibited the lowest affinity for Id1, while the peptide 3CA3 exhibited the higher affinity for Id1, indicating the N-termini position of Tyr1, Ile2 and Gln6 position of peptide **3C** for binding with Id1 are important.

Table 2-4. Peptide sequences and physicochemical characterization of alanine-scanned peptides

Peptide	Peptide sequences	RP-HPLC (Rt, min)	Theoretical MS (Daltons)	MALDI-TOF (Daltons)
3C-A1	AIEGLQALLRDQC	19.1	1428.6	1428.7
3C-A2	YAEGLQALLRDQC	14.1	1478.6	1479.2
3C-A3	YIAGLQALLRDQC	18.6	1462.7	1462.4
3C-A4	YIEALQALLRDQC	17.88	1534.7	1535.2
3C-A5	YIEGAQALLRDQC	12	1478.6	1478.9
3C-A6	YIEGLAALLRDQC	14.6	1463.6	1464.1

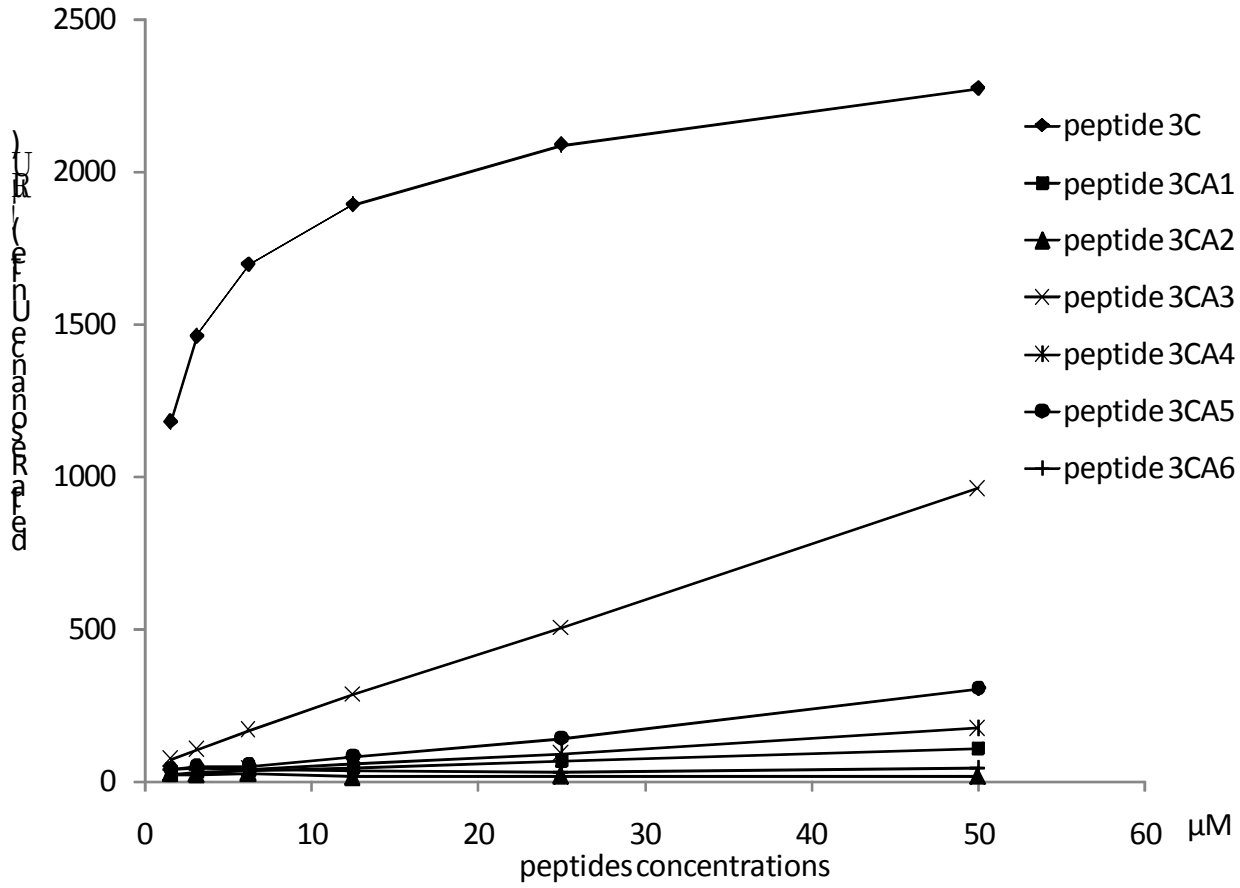

Figure 2-11. Association to the Id1 ligand of six alanine replaced peptide **3C** analogs by SPR method in aqueous buffered solution (pH 7.5).

Discussion

Id proteins play an important role in the generation of blood vessels, the growth of primary, as well as metastatic tumors, thus, we selected Id1 protein as the target for the development of antiproliferative/antitumor agents in this study.

A classic strategy to identify small molecules that specifically target functional Id activities is to use high-throughput screening of large collections of chemical and natural compound libraries, in combination with validated cell-based or cell-free assays. Results of these assays identified the Id associated bHLH partners, including MyoD [33], E2A [34], E47 [35, 36] and E proteins [36]. Accordingly, the *in vitro* studies indicated that MyoD directly binds to Id1 [29, 30] and there is a stronger affinity between MyoD/Id1 than the affinity between MyoD/E47. More recent *in vivo* investigations demonstrated that the critical interactions are between E2A/Id1 and MyoD/E2A [37]. These studies not only demonstrated the E2A/Id1 interaction is stronger than the MyoD/E2A interaction, but also demonstrated the affinity between MyoD/Id1 is stronger than the affinity between MyoD/E2A. Based on these results, we expect that MyoD can associate with Id1 and interrupt interactions involved Id1, therefore, we selected MyoD as our target protein-template and designed three peptide fragments of MyoD (Figure 2-2) which contain the basic, the helix1 and helix2 regions of MyoD in order to investigate the important region of MyoD for binding to Id1 by the SPR-based method. Our goal is to inhibit the proliferation of cancer cells by interrupting the interactions of Id1 with DNA-binding proteins (Figure 2-1), however, on the basis of the studies by Lingbeck *et al.* [37], we can not rule out that our designed peptides may not only disrupt the interaction between Id1 and MyoD but also disrupt the interaction between Id1 and E2A.

SPR results demonstrated that peptides **1A**, **2A**, and **3A** interacted with the immobilized Id1, but exhibited different binding potency for Id1 and showed

significantly different binding profiles (Figure 2-3). The differences in the association and dissociation phases of the binding curves demonstrated that each peptide exhibited different binding potency for Id1 and the peptide **3A** exhibited the highest binding potency for Id1, indicating the importance of the helix2 region of MyoD (the peptide **3A**) for binding to Id1 (Figure 2-3). We believe that the helix2 region of MyoD is crucial for associating with Id1 and this result may explain the binding affinity of MyoD for Id1 [33].

Three smaller, N-terminal deleted peptide analogs of our lead peptide **3A** (**3B**, **3C**, and **3D)** were designed (Figure 2-4), synthesized, and characterized (Table 2-1) for determining their affinity for Id1 by the SPR technology (Figure 2-5 and Table 2-2). It is not surprising that the dissociation constant (K_D) of the most potent peptide **3C** (12.5 μM) is greater than the dissociation constant published for HLH oligomers MyoD/Id (0.7 μM) [29], because the shorter peptide fragments of MyoD may lose some nonconvalent interactions with Id1 due to the deletion of some crucial amino acid residues in MyoD for binding to Id1. Comparing to the numbers of amino acid residues in MyoD protein**,** there is only 13 amino acid residues in **3C,** but the peptide **3C** still exhibited comparable affinity for Id1 (K_D of MyoD vs. K_D of **3C**, 0.7 μM vs. 12.5 μM, respectively), demonstrating the potential of the peptide **3C** as an antagonist of Id1. Thus, the high-affinity peptide **3C** becomes our lead for future design and development of antagonists of Id1 as promising antiproliferative agents by interrupting the Id1-involved interactions.

The SPR-based method established in this study can not only monitor the real-time interaction of each peptide with Id1, but also is useful for screening compounds with high affinity for the immobilized Id1. The SPR-derived K_D value provide an indication of the ability of peptides to bind to Id1 protein *in vitro*, which is informative for further studies of structure-activity relationship, however, this measurement may not reflect

their biological effects in the intact cells.

In order to investigate effects of the secondary structure of each peptide on their affinity for Id1, circular dichroism (CD) spectroscopy was applied to characterize the conformations of peptides **3A**, **3B**, **3C,** and **3D** (Figure 2-6). Results of CD indicate that the presence of 8.42%, 15.43%, and 8.41% helix in **3A**, **3B,** and **3C,** respectively. These results suggest that the lowest affinity of the peptide **3D** (K_D = 367.2 μM) may be due to the absence of the important helical conformation for binding to Id1, and some or all of the first six N-terminal amino acid residues of **3C** (Figure 2-4) are essential for the formation of the helical structure. Although the helical structure is presented in **3A**, **3B,** and **3C**, the affinity of each peptide for Id1 (K_D = 30.6 μM, 38.4 μM, and 12.5 μM, respectively) is not correlated with the contents of the helical structures contained in **3A**, **3B,** and **3C** (8.42%, 15.43%, and 8.41%, respectively). Comparing the results of SPR-based method with the results of CD spectroscopy, we conclude that the high affinity of **3C** for Id1 is caused by not only the presence of the helical structure, but also the presence of the essential amino acid residues for interacting with Id1.

The high affinity of **3C** for Id1 may not reflect its biological effects in the intact cells, therefore, we investigate effects of **3C** in various intact cancer cells by treatment of cancer cells with various concentrations of **3C** and assayed for determination of IC_{50} value of **3C** for the treated-cancer cells (Table 2-3). The IC_{50} value of **3C** determined in HT-29, MCF-7, HL-60, and HCT116 cancer cells are 25 μM, 25 μM, 30 μM and 30 μM, respectively, confirming the antiproliferative effects of **3C** in these intact cancer cells.

Results of our assays demonstrate that treatment of human colon or breast cancer cells with peptide **3C** caused decreased viability of both cancer cells in dose-dependent and time-dependent manners. Because previous studies indicated that Id1 was overexpressed in breast cancer and colorectal adenocarcinoma [38-40], we hypothesize

that the inhibitory effect of peptide **3C** in the proliferation of both cancer cells may be due to its interruption of the interactions of Id1 protein.

Gupta *et al.* demonstrated that *Id* genes mediate tumor reinitiation and implicate breast cancer lung metastasis [41]. Minni *et al.* identified a set of candidate metastasis genes whose expression in primary breast tumors is associated with a high risk of metastasis to the lungs [42], suggested the proliferative mechanisms that initiate metastatic colonization, and implicated Id1 and Id3 as mediators of this malignant function in the TN subgroup of breast cancers. Thus, we investigate the inhibitory effect of **3C** on the proliferation of the invasive cells (lung metastatic MDA-MB-231 cells with aggressive Id1 expression) (Figure 2-8) and found that the IC_{50} of peptide **3C** on TN subgroup invasive cell MDA-MB-231 (60 μM, 48 hr-treatment) were higher than MCF-7 (25 μM, 48 hr-treatment), HL-60 (30 μM, 48 hr-treatment) and HCT116 cancer cells (30 μM, 48 hr-treatment). These results suggested that the peptide **3C** may affect the cell proliferation on overexpressive *Id* gene but lacking expression of estrogen receptor of human breast cancer.

We have demonstrated that our synthetic peptides **3C** exhibited inhibitory effects in the proliferation of HT-29 colon cancer cells and MCF-7 breast cancer cells. Because the expression of Id proteins in various human primary tumor tissues obtained from biopsies have been analyzed [13] and it was reported that Id1 express particularly on human primary tumors such as colorectal carcinoma and breast cancer cells, we suggest that the antiproiferative effects of peptide **3C** in colon cancer cells and breast cancer cells may be due to the interruption of Id1 protein interactions by **3C**. The peptide **3C** exhibited inhibitory effects not only in the proliferation of HT-29 colon cancer cells and MCF-7 breast cancer cells but also in the proliferation of HL-60 leukemia cells and HCT116 colon cancer cells (Table 2-3), indicating the selectivity of **3C** for the Id1-overexpressed cancer cells.

To evaluate the potential of 3C as an antiproliferative agent, we not only screened the selectivity of **3C** among various cancer cells, but also assay the cytotoxicity of **3C** on non-cancer cells (human skin cells, HS-68). Results indicated that even by treatment of HS-68 with 100 μM of peptide **3C** for 24 hrs and 48 hrs, the inhibitory effect of peptide **3C** on the proliferation of HS-68 cells was not detected (Figure 2-9), indicating the peptide **3C** exhibited the specificity for cancer cells.

To confirm the inhibition of proliferation of cancer cells is due to the induced apoptosis of cancer cells instead of necrosis, we analyzed the DNA contents and the apoptotic cells of the peptide **3C**-treated cancer cells by flow cytometry. The peptide **3C**-treated MCF-7 cells showed a decreased G0/G1 phase and an increased sub-G1 peak in the cell cycle (Figure 2-10), indicating the induction of apoptosis of cancer cells by the treatment of cancer cells with 5 μM of peptide **3C** for 24 hrs and 48 hrs and the percentage of cells in G2/M phase increased markedly from 23.34% to 36.43% after incubation for 48 hrs. These results are in agreement with the MTT results, indicating the antipoliferative effect of **3C** on breast cancer cells was correlated with its induction of apoptosis. It also indicated that the peptide **3C** arrested at the G2/M phase of the cell cycle in MCF-7 cancer cells.

In general, alpha-helical conformations in proteins depend in large part on the amino acid residues within the helix and their proximal interactions. For example, an alanine residue has a high propensity to adopt an alpha-helical conformation, whereas that of a glycine residue is low. The preference of peptide **3C** sequence for Id1 heterodimerization is important obviously. In order to identify which residue influence the binding conformation to Id1, alanine was replaced the N1 to N6 position (Table 2-4) and compared their binding affinities to peptide **3C** for Id1 (Figure 2-11). Results showed peptide 3CA2 (YAEGLQALLRDQC) interact Id1 with lowest slope and R^2 = 0.5, indicating an important binding site at N2 of peptide **3C**. Similar to the N2 position,

N6 Ala-replaced peptide (peptide 3CA6, YIEGLAALLRDQC) shows smaller slope than peptide **3C**. We suggest Ile that provide more hydrophobic and steric effect on the binding of ligands to the Id1. In addition, peptide 3CA1 (Tyr1 →Ala), peptide 3CA4 (Gly4 →Ala) and peptide 3CA6 (Gln6 →Ala) associate weakly to Id1, the replaced sequence residues are polar and uncharged characters. These three amino acids are relatively hydrophilic residues and suggest that these positions are important to bind Id1 by forming hydrogen bonds. Furthermore, these irreplaceable residues maybe provide peptide **3C** a rigid conformation for association with Id1.

In conclusion, to our knowledge, this work is the first one that reports not only studies of binding interactions between peptide fragments of MyoD and the Id1 protein, but also bioassays of effects of peptide analogs in various cancer cells. The peptide **3C** inhibited the proliferation of several cancer cells, and results of the SPR study are in agreement with what we expect, the interactions of Id1 were interrupted by designed peptide analogs. Our findings should provide important insights into the development of antiproliferative agents.

References

1. Barone, M. V.; Pepperkok, R.; Peverali, F. A.; Philipson, L. Id proteins control growth induction in mammalian cells. Proc Natl Acad Sci U S A 1994; **91**: 4985-4988.
2. Hara, E.; Yamaguchi, T.; Nojima, H.; Ide, T.; Campisi, J.; Okayama, H.; Oda, K. Id-related genes encoding helix-loop-helix proteins are required for G1 progression and are repressed in senescent human fibroblasts. J Biol Chem 1994; **269**: 2139-2145.
3. Lyden, D.; Young, A. Z.; Zagzag, D.; Yan, W.; Gerald, W.; O'Reilly, R.; Bader, B. L.; Hynes, R. O.; Zhuang, Y.; Manova, K.; Benezra, R. Id1 and Id3 are required for neurogenesis, angiogenesis and vascularization of tumour xenografts. Nature 1999; **401**: 670-677.
4. Mori, S.; Nishikawa, S. I.; Yokota, Y. Lactation defect in mice lacking the helix-loop-helix inhibitor Id2. Embo J 2000; **19**: 5772-5781.
5. Iavarone, A.; Garg, P.; Lasorella, A.; Hsu, J.; Israel, M. A. The helix-loop-helix protein Id-2 enhances cell proliferation and binds to the retinoblastoma protein. Genes Dev 1994; **8**: 1270-1284.
6. Lasorella, A.; Uo, T.; Iavarone, A. Id proteins at the cross-road of development and cancer. Oncogene 2001; **20**: 8326-8333.
7. Norton, J. D. ID helix-loop-helix proteins in cell growth, differentiation and tumorigenesis. J Cell Sci 2000; **113 (Pt 22)**: 3897-3905.
8. Sikder, H. A.; Devlin, M. K.; Dunlap, S.; Ryu, B.; Alani, R. M. Id proteins in cell growth and tumorigenesis. Cancer Cell 2003; **3**: 525-530.
9. Coppe, J. P.; Smith, A. P.; Desprez, P. Y. Id proteins in epithelial cells. Exp Cell Res 2003; **285**: 131-145.
10. Zebedee, Z.; Hara, E. Id proteins in cell cycle control and cellular senescence. Oncogene 2001; **20**: 8317-8325.
11. Ruzinova, M. B.; Benezra, R. Id proteins in development, cell cycle and cancer. Trends Cell Biol 2003; **13**: 410-418.
12. Alani, R. M.; Hasskarl, J.; Grace, M.; Hernandez, M. C.; Israel, M. A.; Munger, K. Immortalization of primary human keratinocytes by the helix-loop-helix protein, Id-1. Proc Natl Acad Sci U S A 1999; **96**: 9637-9641.
13. Fong, S.; Debs, R. J.; Desprez, P. Y. Id genes and proteins as promising targets in cancer therapy. Trends Mol Med 2004; **10**: 387-392.
14. Iavarone, A.; Lasorella, A. ID proteins as targets in cancer and tools in neurobiology. Trends Mol Med 2006; **12**: 588-594.
15. Kim, H.; Chung, H.; Kim, H. J.; Lee, J. Y.; Oh, M. Y.; Kim, Y.; Kong, G. Id-1 regulates Bcl-2 and Bax expression through p53 and NF-kappaB in MCF-7 breast cancer cells. Breast Cancer Res Treat 2008; **112**: 287-296.
16. Meteoglu, I.; Meydan, N.; Erkus, M. Id-1: regulator of EGFR and VEGF and

potential target for colorectal cancer therapy. J Exp Clin Cancer Res 2008; **27**: 69.
17. Benezra, R.; Davis, R. L.; Lockshon, D.; Turner, D. L.; Weintraub, H. The protein Id: a negative regulator of helix-loop-helix DNA binding proteins. Cell 1990; **61**: 49-59.
18. Christy, B. A.; Sanders, L. K.; Lau, L. F.; Copeland, N. G.; Jenkins, N. A.; Nathans, D. An Id-related helix-loop-helix protein encoded by a growth factor-inducible gene. Proc Natl Acad Sci U S A 1991; **88**: 1815-1819.
19. Jen, Y.; Manova, K.; Benezra, R. Expression patterns of Id1, Id2, and Id3 are highly related but distinct from that of Id4 during mouse embryogenesis. Dev Dyn 1996; **207**: 235-252.
20. Jen, Y.; Manova, K.; Benezra, R. Each member of the Id gene family exhibits a unique expression pattern in mouse gastrulation and neurogenesis. Dev Dyn 1997; **208**: 92-106.
21. Moldes, M.; Boizard, M.; Liepvre, X. L.; Feve, B.; Dugail, I.; Pairault, J. Functional antagonism between inhibitor of DNA binding (Id) and adipocyte determination and differentiation factor 1/sterol regulatory element-binding protein-1c (ADD1/SREBP-1c) trans-factors for the regulation of fatty acid synthase promoter in adipocytes. Biochem J 1999; **344 Pt 3**: 873-880.
22. Roberts, E. C.; Deed, R. W.; Inoue, T.; Norton, J. D.; Sharrocks, A. D. Id helix-loop-helix proteins antagonize pax transcription factor activity by inhibiting DNA binding. Mol Cell Biol 2001; **21**: 524-533.
23. Perk, J.; Iavarone, A.; Benezra, R. Id family of helix-loop-helix proteins in cancer. Nat Rev Cancer 2005; **5**: 603-614.
24. Henke, E.; Perk, J.; Vider, J.; de Candia, P.; Chin, Y.; Solit, D. B.; Ponomarev, V.; Cartegni, L.; Manova, K.; Rosen, N.; Benezra, R. Peptide-conjugated antisense oligonucleotides for targeted inhibition of a transcriptional regulator in vivo. Nat Biotechnol 2008; **26**: 91-100.
25. Lung, F. D.; Tsai, J. Y.; Wei, S. Y.; Cheng, J. W.; Chen, C.; Li, P.; Roller, P. P. Novel peptide inhibitors for Grb2 SH2 domain and their detection by surface plasmon resonance. J Pept Res 2002; **60**: 143-149.
26. Merrifield, R. B. Solid-phase peptide synthesis. Adv Enzymol Relat Areas Mol Biol 1969; **32**: 221-296.
27. Lung, F. D.; Chen, H. Y.; Lin, H. T. Monitoring bone loss using ELISA and surface plasmon resonance (SPR) technology. Protein Pept Lett 2003; **10**: 313-319.
28. Lung, F. D.; Tsai, J. Y. Grb2 SH2 domain-binding peptide analogs as potential anticancer agents. Biopolymers 2003; **71**: 132-140.
29. Fairman, R.; Beran-Steed, R. K.; Anthony-Cahill, S. J.; Lear, J. D.; Stafford, W. F., 3rd; DeGrado, W. F.; Benfield, P. A.; Brenner, S. L. Multiple oligomeric states regulate the DNA binding of helix-loop-helix peptides. Proc Natl Acad Sci U S A 1993; **90**:

10429-10433.
30. Pesce, S.; Benezra, R. The loop region of the helix-loop-helix protein Id1 is critical for its dominant negative activity. Mol Cell Biol 1993; **13**: 7874-7880.
31. Perez-Iratxeta, C.; Andrade-Navarro, M. A. K2D2: estimation of protein secondary structure from circular dichroism spectra. BMC Struct Biol 2008; **8**: 25.
32. Wilson, J. W.; Deed, R. W.; Inoue, T.; Balzi, M.; Becciolini, A.; Faraoni, P.; Potten, C. S.; Norton, J. D. Expression of Id helix-loop-helix proteins in colorectal adenocarcinoma correlates with p53 expression and mitotic index. Cancer Res 2001; **61**: 8803-8810.
33. Jan, Y. N.; Jan, L. Y. Functional gene cassettes in development. Proc Natl Acad Sci U S A 1993; **90**: 8305-8307.
34. Neuhold, L. A.; Wold, B. HLH forced dimers: tethering MyoD to E47 generates a dominant positive myogenic factor insulated from negative regulation by Id. Cell 1993; **74**: 1033-1042.
35. Quesenberry, P. J.; Iscove, N. N.; Cooper, C.; Brady, G.; Newburger, P. E.; Stein, G. S.; Stein, J. S.; Reddy, G. P.; Pearson-White, S. Expression of basic helix-loop-helix transcription factors in explant hematopoietic progenitors. J Cell Biochem 1996; **61**: 478-488.
36. Spicer, D. B.; Rhee, J.; Cheung, W. L.; Lassar, A. B. Inhibition of myogenic bHLH and MEF2 transcription factors by the bHLH protein Twist. Science 1996; **272**: 1476-1480.
37. Lingbeck, J. M.; Trausch-Azar, J. S.; Ciechanover, A.; Schwartz, A. L. In vivo interactions of MyoD, Id1, and E2A proteins determined by acceptor photobleaching fluorescence resonance energy transfer. Faseb J 2008; **22**: 1694-1701.
38. Fong, S.; Itahana, Y.; Sumida, T.; Singh, J.; Coppe, J. P.; Liu, Y.; Richards, P. C.; Bennington, J. L.; Lee, N. M.; Debs, R. J.; Desprez, P. Y. Id-1 as a molecular target in therapy for breast cancer cell invasion and metastasis. Proc Natl Acad Sci U S A 2003; **100**: 13543-13548.
39. Lin, C. Q.; Singh, J.; Murata, K.; Itahana, Y.; Parrinello, S.; Liang, S. H.; Gillett, C. E.; Campisi, J.; Desprez, P. Y. A role for Id-1 in the aggressive phenotype and steroid hormone response of human breast cancer cells. Cancer Res 2000; **60**: 1332-1340.
40. Schoppmann, S. F.; Schindl, M.; Bayer, G.; Aumayr, K.; Dienes, J.; Horvat, R.; Rudas, M.; Gnant, M.; Jakesz, R.; Birner, P. Overexpression of Id-1 is associated with poor clinical outcome in node negative breast cancer. Int J Cancer 2003; **104**: 677-682.
41. Gupta, G. P.; Perk, J.; Acharyya, S.; de Candia, P.; Mittal, V.; Todorova-Manova, K.; Gerald, W. L.; Brogi, E.; Benezra, R.; Massague, J. ID genes mediate tumor reinitiation during breast cancer lung metastasis. Proc Natl Acad Sci U S A 2007; **104**: 19506-19511.

42. Minn, A. J.; Gupta, G. P.; Siegel, P. M.; Bos, P. D.; Shu, W.; Giri, D. D.; Viale, A.; Olshen, A. B.; Gerald, W. L.; Massague, J. Genes that mediate breast cancer metastasis to lung. Nature 2005; **436**: 518-524.

Chapter 3

In processing and future works

These years, we focus on developing peptidic inhibitors of the Grb2 SH2 domain as promising anticancer agents. However, cell membrane constitutes a serious barrier for protecting the integrity of cells, it may limit the effectiveness of peptidic inhibitors as anti-cancer drugs. In Grb2 SH2 study, to enhance the cell permeability of peptides, we designed two peptide analogs by incorporation of the cell-penetrating peptide (CPP) onto one of our leading peptide inhibitors of Grb2-SH2, Fmoc-Glu-Tyr-Aib-Asn-NH_2. These cell-penetrating peptides include HIV Tat-derived peptide and the cytostatic agent methotrexate sequence. The binding interaction between each synthetic peptide and Grb2 SH2 domain was detected by using the surface plasmon resonance (SPR) technology developed with the BIAcore-biosensor. We also investigated the biological activities of each peptide in human breast cancer cells. Effects of peptides on the cell cycle progression and apoptosis in cancer cell were studied by flow cytometry. In addition, we also integrated the novel fluorescent amino acid to investigate the effect for cell penetrating under laser scanning confocal microscope.

Recently, we have designed a series of peptidic inhibitors of Id1 on the basis of the sequence of a helix region of *Myo*D. Peptides were synthesized by solid phase peptide synthesis, purified by RP-HPLC, and characterized by MALDI-TOF Mass spectrometer. Effects of synthetic peptides on breast and colony cancer cells were investigated. Biological results showed that among the synthesized peptides, the peptide **3C** (the amino acid sequence: H-Tyr-Ile-Glu-Gly-Leu-Gln-Ala-Leu-Leu-Arg-Asp-Gln-NH_2) exhibited the strongest antiproliferative effects on MCF-7 and HT-29 cells with the IC_{50} value of 20 μM, respectively. In-processing objective of this project is to design and synthesize the N- and C-terminal deleted analogs of **3C**, and to investigate the biological effects of these peptide analogs on breast and colony cancer cells. Effects of

peptides on the cell proliferation and the progression of cell cycle of cancer cells will be evaluated using *in vitro* bioassays. Potent linear peptides will be further designed for cyclization to enhance their stability and potency. The potent peptides will be co-crystallized with Id protein and the conformation of peptide/Id complex will be established by X-ray crystallography. The bioactive conformation of peptide/Id complex will be established by using molecular modeling tool, 3D-QSAR. In addition, the metal-chelated functional peptide analogs which containing in the peptide **3C** can selectively bind to Id1. We expect these novel peptides may target on and hydrolyze Id1, such function as the Id1 protease or Id1 peptidase. Results of this project should be very useful for the development of anticproliferative agents.